UNIVERSIDADE DA BEIRA INTERIOR
Ciências da Saúde

Design of an one-step platform purification of STEAP1 using Hydrophobic Interaction Chromatography

Diogo José Pinheiro Monteiro

Dissertação para obtenção do grau de Mestre em
Ciências Biomédicas
(2º Ciclo de estudos)

Orientador: Prof. Doutor Luís António Paulino Passarinha
Co-orientador: Prof. Doutor Cláudio Jorge Maia Batista

Covilhã, junho de 2018

Acknowledgements

Firstly, I would like to make special thanks to my supervisors, Professor Luís Passarinha and Professor Cláudio Maia for the opportunity that was given to me to demonstrate my worth and work developing this work. Thank you also for all the time you have given for my guidance and for all the advice and reviews that have helped to greatly improve this dissertation. Also, to all my colleagues and friends at CICS, thank you for the friendship, support, mutual help, patience and encouragement. Special thanks to Fátima Santos, Diana Duarte and Jorge Ferreira for the main help, friendship, and teachings during the last year.

To all my dear friends from all over the world a huge thank for all the support and care. Friends with whom I shared the best and the worst moments of my life, helping me to relax and believe in a better future giving me an extra motivation. Also, a huge thank to all my cyclist friends to be an important daily distraction outdoor the lab, being the competition and sport a great school for life, teaching above all the highest ethical values.

My forever thankfulness goes to my family, especially my mom and dad, for whom I have the greatest respect and love in the world, for the fact that they have been present throughout my all life. They give me with much effort, the possible and the impossible, to get where I came and show with pride the person that I am today. This dissertation is entirely dedicated to you all.

Resumo

O cancro de próstata é um dos carcinomas mais letais e prevalentes entre homens idosos em todo o mundo. Atualmente, o diagnóstico do cancro da próstata baseado nos níveis de *Prostate Specific Antigen (PSA)* é inespecífico e com eficiência limitada, principalmente em estágios avançados de cancro. Assim, existe a necessidade de identificar e caracterizar biomarcadores proteicos específicos e confiáveis para o cancro da próstata. *A Six-transmembrane Epithelial Antigen of the Prostate* 1 (STEAP1) é uma proteína transmembranar cujos altos níveis de expressão foram correlacionados com o cancro da próstata. A STEAP1 pode participar na comunicação intracelular e intercelular em células cancerígenas através da modulação da proliferação celular e invasão tumoral através da sua potencial atividade como canal iónico ou transportador. Assim, a caracterização da estrutura da STEAP1 pode permitir a conceção de inibidores específicos que diminuem e modulam a sua função oncogénica. Os estudos estruturais e funcionais requerem quantidades elevadas de proteína purificada, que podem ser obtidas através de uma produção recombinante da proteína STEAP1 humana integrada com uma estratégia cromatográfica adequada. Neste trabalho, foi avaliado o desempenho da Octil- e Butyl-Sepharose de acordo com as condições de ligação e eluição necessárias para o isolamento da STEAP1 a partir de lisados celulares, obtidos em culturas induzidas com metanol num mini biorreator de *Pichia pastoris* X33. A concentração do tampão fosfato de sódio e fosfato monossódico com cloreto de sódio no tampão de equilíbrio foi otimizada para promover uma adsorção completa da STEAP1 nos suportes hidrofóbicos. Sucintamente, observou-se uma retenção mais elevada da STEAP1 com concentrações acima de 500 mM de tampão fosfato de sódio e fosfato monossódico com cloreto de sódio, pH 8,0. Se a adsorção for alcançada com altas concentrações de tampão fosfato de sódio ou fosfato monossódico com cloreto de sódio, a eluição deve ser realizada com concentrações crescentes de Triton X-100 em 50 mM de tampão fosfato. Os resultados obtidos indicam que a exposição dos domínios de ligação de membrana da STEAP1 à Octyl- e Butyl-Sepharose requerem à priori altas concentrações de sal devido às fortes interações estabelecidas entre eles. No entanto, após a sua adsorção completa, a eluição da STEAP1 requer agentes caotrópicos, como detergentes. Embora a aplicação da Cromatografia de Interação Hidrofóbica (HIC) na purificação de proteínas integrais de membrana seja incomum, os resultados obtidos no desenvolvimento da dissertação indicam que a utilização de matrizes hidrofóbicas tradicionais pode abrir uma alternativa promissora para o isolamento da STEAP1 a partir de lisados celulares.

Palavras-chave

Cromatografia de Interação Hidrofóbica, Cancro da Próstata, Purificação, STEAP1.

Resumo Alargado

O cancro de próstata é um dos carcinomas mais letais e prevalentes entre homens idosos em todo o mundo, apresentando especial incidência em homens com idade superior a 50 anos. Atualmente, os meios de diagnóstico e terapia existentes do cancro da próstata, principalmente em estágios avançados de cancro, são invasivos, inespecíficos e com eficiência limitada, sendo predominantemente baseados nos níveis de *Prostate Specific Antigen (PSA)*. Assim, existe a necessidade de identificar e caracterizar biomarcadores proteicos específicos e confiáveis para o cancro da próstata. *The Six-transmembrane Epithelial Antigen of the Prostate* 1 (STEAP1) é uma proteína constituída por seis domínios transmembranares interligados por *loops* extracelulares, geralmente localizada na membrana plasmática, cujos altos níveis de expressão foram correlacionados com o cancro da próstata. A STEAP1 pode participar na comunicação intracelular e intercelular em células cancerígenas através da modulação da proliferação celular e invasão tumoral através da sua potencial atividade como canal iónico ou transportador. Assim, a caracterização da estrutura da STEAP1 pode permitir a conceção de inibidores específicos que diminuem e modulam a sua função oncogénica, permitindo a sua utilização como alvo terapêutico. Os estudos estruturais e funcionais requerem quantidades elevadas de proteína purificada, que podem ser obtidas através de uma produção recombinante da proteína STEAP1 humana integrada com uma estratégia cromatográfica adequada. Assim, o principal objetivo desta tese de mestrado foi desenvolver uma estratégia cromatográfica sustentável de um passo para a purificação da STEAP1, recuperada a partir de lisados de *Pichia pastoris*, usando a Cromatografia de Interação Hidrofóbica. Para atingir este objetivo final, vários procedimentos foram desenvolvidos e otimizados, tais como: a) Otimização do processo de recuperação de lisados de *Pichia pastoris* através da determinação do detergente mais eficaz para a solubilização da STEAP1; b) Desenvolvimento de um procedimento por Cromatografia de Interação Hidrofóbica através da avaliação do desempenho da Octyl- e Butyl-Sepharose de acordo com as condições requeridas para a ligação e eluição da STEAP1 nestas matrizes. A proteína STEAP1 foi obtida através de produção recombinante realizada em mini-biorreator de culturas de *Pichia pastoris X33 Mut*$^{+}$. Fundamentalmente o processo fermentativo compreende três fases principais: fase batch de glicerol, fed-batch e indução com metanol. Assim, como já otimizado pelo nosso grupo de trabalho, a melhor estratégia para a obtenção da proteína com menor agregação é a fermentação com 20 horas de um batch de glicerol, seguida de 3 horas de fed-batch e posterior indução com metanol durante 10 horas. O passo seguinte consistiu em isolar o péptido de interesse no seu estado nativo adotando o método de lise por esferas, sendo que na etapa de solubilização, de entre cinco detergentes (SDS, Twenn-20, Tween-80, NP-40, Triton X-100 e CHAPS) foi estabelecido que o Triton X-100 alcançou o resultado mais eficiente, preservando a estrutura nativa da STEAP1 com os padrões de expressão mais elevados. Na etapa de purificação, a concentração do tampão fosfato de sódio e fosfato monossódico com cloreto de sódio no tampão de equilíbrio foi otimizada para promover uma adsorção completa da STEAP1 nos suportes hidrofóbicos. Observou-se uma retenção mais elevada da STEAP1 com concentrações acima de 500 mM de tampão fosfato de

sódio e fosfato monossódico com cloreto de sódio, pH 8,0. Se a adsorção for alcançada com altas concentrações de tampão fosfato de sódio ou fosfato monossódico com cloreto de sódio, a eluição deve ser realizada com concentrações crescentes de Triton X-100 em 50 mM de tampão fosfato. Os resultados obtidos indicam que a exposição dos domínios de ligação de membrana da STEAP1 à Octyl- e Butyl-Sepharose requerem à priori altas concentrações de sal devido às fortes interações estabelecidas entre eles. No entanto, após a sua adsorção completa, a eluição da STEAP1 requer agentes caotrópicos, como detergentes. Embora a aplicação da Cromatografia de Interação Hidrofóbica (HIC) na purificação de proteínas integrais de membrana seja incomum, os resultados obtidos no desenvolvimento da dissertação indicam que a utilização de matrizes hidrofóbicas tradicionais pode abrir uma alternativa promissora para o isolamento da STEAP1 a partir de lisados celulares.

Abstract

Prostate cancer is one of the most lethal and prevalent carcinoma among elder men worldwide. Currently, prostate cancer diagnosis based on prostate-specific antigen levels is unspecific and with limited efficient, mainly in advanced stages of cancer. Thus, there is a need to identify and characterize specific and reliable protein biomarkers for prostate cancer. Six transmembrane epithelial antigen of the prostate 1 (STEAP1) is a transmembrane protein whose high expression levels were correlated with PCa. STEAP1 may take part in intracellular and intercellular communication in cancer cells by modulating cell proliferation and tumor invasiveness through its potential activity as ion channel or transporter. So, the characterization of STEAP1 structure might allow the design of specific inhibitors that decrease and modulate its oncogenic function. The structural and functional studies require high purified amounts of protein, which can be obtained through a recombinant production of human STEAP1 protein integrated with a properly chromatographic strategy. In this work, the performance of Octyl- and Butyl-Sepharose were evaluated according to binding and elution conditions required for STEAP1 isolation from cell lysates, obtained in mini-bioreactor *Pichia pastoris* X33 methanol-induced cultures. The concentration of sodium phosphate buffer and monosodium phosphate plus sodium chloride in the equilibration buffer was optimized in order to promote a complete STEAP1 adsorption on the hydrophobics supports. Succinctly, a higher retention of STEAP1 was observed with concentrations above 500 mM of sodium phosphate buffer and monosodium phosphate plus sodium chloride, pH 8.0. If the adsorption is achieved at high concentrations of sodium phosphate buffer, the elution must be performed with increasing concentrations of Triton X-100 in 50 mM phosphate buffer. The obtained results indicate that the exposition of membrane binding domains of STEAP1 to Octyl- and Butyl- Sepharose requires high salt concentrations due the strong interactions established between them. However, after its complete adsorption, STEAP1 elution requires chaotropic agents such as detergents. Although application of HIC in the purification of integral membrane proteins are uncommon, the obtained results in the development of this dissertation indicate that the use of traditional hydrophobic matrices may open a promising alternative for the isolation of STEAP1 from cell lysates.

Keywords

Hydrophobic Interaction Chromatography, Prostate Cancer, Purification, STEAP1.

Index

List of Figures

Figure 10. BSA calibration curve for total protein quantification (µg/mL) ranged between 25 –2000 µg/mL.

Figure 11. Western blot analysis of the STEAP1 solubilization using 1% (v/v) of some common detergents applied in the literature.

Figure 12. Schematic structures of Butyl- and Octyl-Sepharose ligands.

Figure 13. Initial purification screening trials on Octyl-Sepharose. (A) sodium chloride; (B) sodium phosphate buffer. Adsorption was performed at salt concentrations of 500 mM (pH 8.0). Desorption was performed with 50 mM sodium phosphate buffer (pH 8.0). Different color lines represent the absorbance at 280 nm, brown line the conductivity and the continuous green line represents sodium phosphate buffer concentration.

Figure 14. Dot blot analysis of samples collected on chromatographic profiles of figure 13. Lane L – Solubilized lysis pellet; Lane I – Peaks I obtained at 500 mM of sodium chloride and sodium phosphate buffer and Lane II – Peak II obtained with 50 mM sodium phosphate buffer on Octyl-Sepharose.

Figure 15. SDS-PAGE (A) and Western blot (B) analysis of samples collected on chromatographic profiles of figure 14. L – Solubilized lysis pellet; Lane I – Peaks I obtained at 500 mM and Lane II – Peak II obtained with 50mM sodium phosphate buffer on Octyl-Sepharose.

Figure 16. Chromatographic profile of STEAP1 isolation trials on Octyl-Sepharose. Adsorption was performed at 750 mM sodium chloride, pH 8.0 followed by 50 mM sodium phosphate buffer step. Blue line represents the absorbance at 280 nm, green line the sodium phosphate buffer concentration in mobile phase, and the brown line the conductivity.

Figure 17. SDS-PAGE (A) and Western Blot (B) analysis of samples collected on STEAP1 isolation chromatographic assay [figure 16]. Lane MW – molecular weight standards; Lane L – solubilized lysis pellet; Lane I – Peaks I obtained at 750 mM sodium chloride; Lane II – Peak II obtained with 50 mM sodium phosphate buffer.

Figure 18. Chromatographic profile of STEAP1 isolation on Octyl-Sepharose. Adsorption was performed at 1000 mM sodium phosphate buffer, pH 8.0 followed by 50 mM sodium phosphate buffer step. Desorption was performed at 1% Triton X-100, pH 8.0. Blue line represents the absorbance at 280 nm, green line the sodium phosphate buffer concentration in mobile phase, red line the Triton X-100 composition in mobile phase and the brown line the conductivity.

Figure 19. SDS-PAGE (A) and Western Blot (B) analysis of samples collected on STEAP1 isolation chromatographic assay [figure 18]. Lane MW – molecular weight standards; Lane L – solubilized lysis pellet; Lane I – Peaks I obtained at 1000 mM sodium chloride; Lane II – Peak II obtained with 50 mM sodium phosphate buffer. Lanes III and IV – Peaks III and IV obtained with a linear gradient of 1% Triton X-100.

Figure 20. Chromatographic profiles of STEAP1 isolation trials on Octyl-Sepharose. Adsorption was performed

at 750 mM monosodium phosphate with sodium chloride, pH 8.0 followed by 50 mM sodium phosphate buffer step. Desorption was performed in linear gradient (A) and step gradient (B) of 1% Triton X-100, pH 8.0. Blue line represents the absorbance at 280 nm, green line the monosodium phosphate with sodium chloride concentration in mobile phase, red line the Triton X-100 percentage in mobile phase and the brown line the conductivity.

Figure 21. SDS-PAGE (A) and Western Blot (B) analysis of samples collected on STEAP1 isolation chromatographic assay [figure 20 (A)]. Lane MW – molecular weight standards; Lane L – solubilized lysis pellet; Lane I – Peaks I obtained at 750 mM monosodium phosphate with sodium chloride; Lane II – Peak II obtained with 50Mm sodium phosphate buffer; Lanes III and IV – Peaks III and IV obtained at linear gradient of 1% Triton X-100.

Figure 22. SDS-PAGE (A) and Western Blot (B) analysis of samples collected on STEAP1 isolation chromatographic assay [figure 20 (B)]. Lane MW – molecular weight standards; Lane L – solubilized lysis pellet; Lane I – Peaks I obtained at 750 mM monosodium phosphate with sodium chloride; Lane II – Peak II obtained with 50Mm sodium phosphate buffer; Lanes III and IV – Peaks III and IV obtained at step gradient of 1% Triton X-100.

Figure 23. Chromatographic profiles of STEAP1 isolation trials on Octyl-Sepharose. Adsorption was performed at 750 mM monosodium phosphate with sodium chloride, pH 8.0 followed by 50 mM sodium phosphate buffer step. Desorption was performed in linear gradient (A) and step gradient (B) of 1% Triton X-100, pH 8.0. Blue line represents the absorbance at 280 nm, green line the monosodium phosphate with sodium chloride concentration in mobile phase, red line the Triton X-100 percentage in mobile phase and the brown line the conductivity.

Figure 24. SDS-PAGE (A) and Western Blot (B) analysis of samples collected on STEAP1 isolation chromatographic assay [figure 23 (A)]. Lane MW – molecular weight standards; Lane L – solubilized lysis pellet; Lane I – Peaks I obtained at 750 mM monosodium phosphate with sodium chloride; Lane II – Peak II obtained with 50 mM sodium phosphate buffer; Lanes III and IV – Peaks III and IV obtained at linear gradient of 1% Triton X-100.

Figure 25. SDS-PAGE (A) and Western Blot (B) analysis of samples collected on STEAP1 isolation chromatographic assay [figure 23 (B)]. Lane MW – molecular weight standards; Lane L – solubilized lysis pellet; Lane I – Peaks I obtained at 750 mM monosodium phosphate with sodium chloride; Lane II – Peak II obtained with 50 mM sodium phosphate buffer; Lanes III and IV – Peaks III and IV obtained at step gradient of 1% Triton X-100.

Figure 26. Chromatographic profile of STEAP1 isolation trial on Butyl-Sepharose (HIC). Adsorption was performed at 800 mM monosodium phosphate with sodium chloride, pH 8.0 followed by 50 mM sodium phosphate buffer step. Desorption was performed with a linear gradient of 1% Triton X-100, pH 8.0. Blue line represents the absorbance at 280 nm, green line the monosodium phosphate with sodium chloride concentration in mobile phase, red line the Triton X-100 percentage in mobile phase and the brown line the conductivity.

Figure 27. SDS-PAGE (A) and Western Blot (B) analysis of samples collected on STEAP1 isolation

chromatographic assay [figure 26]. Lane MW – molecular weight standards; Lane L – solubilized lysis pellet; Lane I – Peaks I obtained at 800 mM monosodium phosphate with sodium chloride; Lane II – Peak II obtained with 50 mM sodium phosphate buffer; Lanes III and IV – Peaks III and IV obtained at linear gradient of 1% Triton X-100.

List of Tables

List of abbreviations

PSA	Prostate Specific Antigen
STEAP1	Six-transmembrane Epithelial Antigen of Prostate 1
HIC	Hydrophobic Interaction Chromatography
CZ	Central Zone
TZ	Transition Zone
PZ	Peripheral Zone
BPH	Benign Prostatic Hyperplasia
PCa	Prostate Cancer
AFMS	Anterior Fibromuscular Stroma
UGS	Urogenital Sinus
UGE	Urogenital Sinus Epithelium
UGM	Urogenital Sinus Mesenchyme
DHT	Androgen 5α-dihydrotestosterone
AR	Androgen Receptor
ROS	Reactive Oxygen Species
ED	Endocrine Disruptors
PIN	Prostatic Intraepithelial Neoplasia
PIA	Proliferative Inflammatory Atrophy
PTEN	Phosphatase and Tensin Homologue
AIPC	Androgen-independent Prostate Cancer
EZH2	Enhancer of Zeste Homolog Gene 2
Upa	Urokinase Plasminogen Activator
TMPRSS2	Transmembrane Protease Serine 2
MCTs	Monocarboxylate Transporters
PCA3	Prostate Cancer Antigen 3
GOLPH2	Golgi Phosphoprotein 2
PTM	Post-translational Modifications
TFR1	Transferrin Receptor 1
TAAS	Tumor-associated Antigens
CTLs	Cytotoxic T Lymphocytes
PDB	Protein Data Bank
SDS	Sodium Dodecyl Sulfate
IMAC	Immobilized Metal-ion Affinity Chromatography
SEC	Size-exclusion Chromatography
IEC	Ion-exchange Chromatography
RPC	Reverse-phase Chromatography
BSA	Bovine Serum Albumin

CV	Column Volume
SDS-PAGE	Sodium Dodecyl Sulphate-Polyacrylamide Gel Electrophoresis
PMSF	Phenylmethylsulphonyl fluoride
hSCOMT	Human Soluble Catechol-O-methyltransferase
hMBCOMT	Human Membrane Bound Catechol-O-methyltransferase

Chapter 1

Introduction

1. Human Prostate

1.1 Anatomy and Physiology

The human prostate is a tubuloalveolar exocrine gland of the male reproductive system. The function of the prostate is to secrete a thin and, slightly alkaline fluid that forms a portion of the seminal fluid, an organic fluid that suspend the ejaculated sperm and maintain their mobility (1). The human adult prostate is a walnut-sized organ measuring 4x3x2 cm in wide, length and height, respectively, and weight of around 20 g. It is located posteriorly to the lower portion of the symphysis pubis, at the base of the urinary bladder, at the apex of the urogenital diaphragm and is separated anteriorly from rectum by the Denonvilliers' fascia [Figure 1(A)]. At histological level, prostate is a branched duct gland with a pseudostratified epithelium composed of three differentiated epithelial cell types: luminal, basal and neuroendocrine. The inner layer of the prostate capsule is composed of smooth muscle with an outer layer covering of collagen (2-4).

McNeal divided the prostate into three major areas that are histologically distinct and anatomically separate, the Central Zone (CZ), Transition Zone (TZ) and Peripheral Zone (PZ) [figure 1(B)] (3). The CZ is a vertical wedge of glandular tissue, like a cone-shaped structure, with approximately 25% of the glandular tissue which surrounds the ejaculatory ducts and constitutes most of the apex of the prostate between the TZ and PZ. TZ is a smaller region with only 5% of the glandular tissue and consists of two equal small lobules portions of glandular tissue lateral to the urethra in the midgland (3) (5). This is the portion of the prostate involved in the development of Benign Prostatic Hyperplasia (BPH) and less commonly adenocarcinoma (1). The PZ is the largest area, comprising 70% of prostate, occupying from the base to the apex along the posterior surface and surrounds the distal urethra. This zone is the main site of prostate cancer (PCa), chronic prostatitis, postinflammatory atrophy and although not of BPH. Some authors also considered a fourth zone in the prostate, the Anterior Fibromuscular Stroma (AFMS) that forms the convexity of the anterior external surface (6). This apical area is rich in striated muscle, which blends into the muscle of pelvic diaphragm. The voluntary sphincter functions are performed by the distal portion of AFMS, while proximal portion plays a central role in involuntary sphincter functions (2) (5-7).

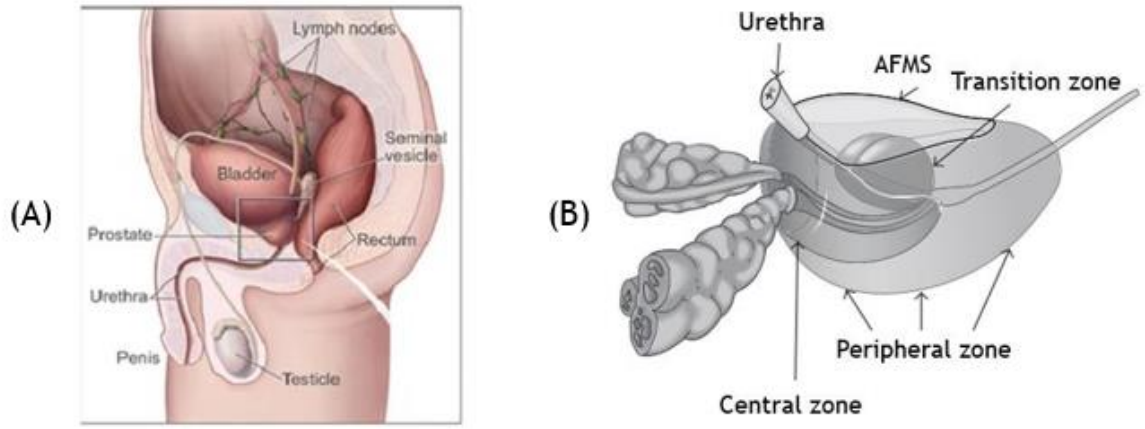

Figure 1. Anatomy of an adult human prostate showing urethra and bladder in relation to the four major glandular regions of the prostate. Central zone (CZ) that surrounds the ejaculatory duct, peripheral zone (PZ) that consists in about 70 % of prostate, and transitional zone (TZ) that surrounds proximal prostatic urethra and the anterior fibromuscular stroma (AFMS), which allows the connection between anterior and apical surfaces (adapted from (8)).

Growth and development of the prostate begin at 10 weeks of gestation in humans, with the formation of prostatic buds from the fetal urogenital sinus (UGS), but only are completed at sexual maturity. The initial event is the outgrowth of solid epithelial buds from the Urogenital Sinus Epithelium (UGE) into the surrounding Urogenital Sinus Mesenchyme (UGM). The influence of testicular androgens is required to the proliferation of prostatic buds to originate solid cords of epithelial cells, which grow into the UGM in a particular spatial arrangement to establish the lobar divisions of the prostate (1). This androgen 5α-dihydrotestosterone (DHT), is synthesized from fetal testosterone by the action of 5α-reductase and is localized in the urogenital sinus and external genitalia of humans (9). Postnatally, under the influence of androgens, the epithelial cells undergo differentiation, produce protein secretions, and express characteristic markers such as cytokeratins 8 and 18, as well as high levels of Androgen Receptor (AR) and PSA. By observation of basal cells, it is possible to differentiate adenocarcinomas from benign conditions, since they are multipotent and can generate all epithelial lineages of prostate. Finally, neuroendocrine cells are rare cells of unclear function that express endocrine markers such as chromogranin A, synaptophysin and PSA, but not AR (10-11).

1.2 Prostate Cancer

1.2.1 Epidemiology

PCa is one of the most lethal and prevalent carcinoma affecting men worldwide and the second leading cause of cancer-related death of men in 2018 (29 430 estimated deaths) (12), with the highest number of new estimated cases (164 690 cases).

The highest prostate cancer incidence rates are found in developed regions, including Western and Northern Europe, Northern America and Australia/New Zeeland, whereas Asian and African countries have lower rates of incidence. The practice of PSA testing is the main reason to this discrepancy in incidence rates, which are able to detect even asymptomatic tumors, and in developing countries biopsy has become available for prostate cancer screening (13).

In Portugal is the main cancer diagnosed in men and the third cause of death. Although the incidence in Portugal is increasing, the mortality associated with prostate cancer seems to be decreasing constantly over the time (14-15).

1.2.2 Risk Factors

Several research studies have given insight into the causes and risk factors for prostate cancer (16-17). Although the specific causes remain unknown, several risk factors have been identified, which may contribute to the initiation and progression of this pathology.

The risk factors can be classified as endogenous or exogenous. In the first group there are factors such as age, family history, race, hormones and oxidative stress. The second group is constituted by diet, environmental agents and occupation (18). The major risk factor for PCa is age, once about 85% of cases are diagnosed after 65 years old (19). Family history can be associated with high risk of PCa, since have long known that cancer susceptibility can be inherited (20). In addition, race is also referred as a risk factor, since African-Americans have twice the risk of non-Hispanic white's due differences in allelic frequencies of microsatellites or polymorphic variations at the AR locus (21-22). Reactive oxygen species (ROS) and the coupled oxidative stress have been associated with tumor formation, as ROS can act as secondary messengers and control several signaling cascades (22-23). High concentrations of sex steroids, in particular androgens such as testosterone and its metabolites, (e.g. dihydrotestosterone) have been implicated in the pathogenesis of prostate cancer (24-25). Fat consumption, especially polyunsaturated fat, shows a strong and positive correlation with prostate cancer incidence and mortality, perhaps resulting from fat-induced alterations in hormonal profiles, in proteins or DNA-reactive intermediates or in increasing of oxidative stress (26-28).The Endocrine Disruptors (ED) are a class of environmental agents which are highly correlated with PCa. An ED can be defined as an environmental agent that positively or negatively alters hormone activity and ultimately leads to effects on reproduction, development, and carcinogenesis, particularly of reproductive organs. Certain pesticide residues on foods, chemicals used in plastics production and phytoestrogens in dietary plant products behave as ED. Exposure to ED can occur through ingestion of food or water or through inhalation (29-31)

Finally, numerous other factors have shown some correlation with PCa, including smoking, energy intake, sexual activity, marital status, vasectomy, social factors (lifestyle, socioeconomic factors, and education), physical activity, and anthropometry (18).

1.2.3 Prostate Carcinogenesis

PCa develops through the accumulation of somatic genetic and epigenetic changes, resulting in the inactivation of tumor suppressor genes and caretaker genes and/or the activation of oncogenes and angiogenesis (32). Prostate cancer occurs when the rate of cell division overcomes cell death, leading to uncontrolled tumor growth. After the initial transformation event, additional mutations of a multitude of genes, including the genes for p53 and retinoblastoma, can result in tumor progression and metastasis (33).

More than 95% of PCa are adenocarcinomas that emerge from prostatic epithelial cells. Of these cases, 70% occur in the PZ, 15-20% in the CZ and 10-15% in the TZ. Most of cancer cells are multifocal and influenced simultaneously by numerous regions of the prostate gland (34). The pathophysiology of PCa englobes benign lesions, namely BPH or malignant, such as Prostatic Intraepithelial Neoplasia (PIN) or adenocarcinoma. Proliferative Inflammatory Atrophy (PIA) is characterized by atrophic lesions in which there is an increase in the fraction of epithelial cells that proliferate in focal atrophy lesions, when compared with normal epithelium (Figure 2) Normally, PIA is identified adjacent to high-grade PIN (35).

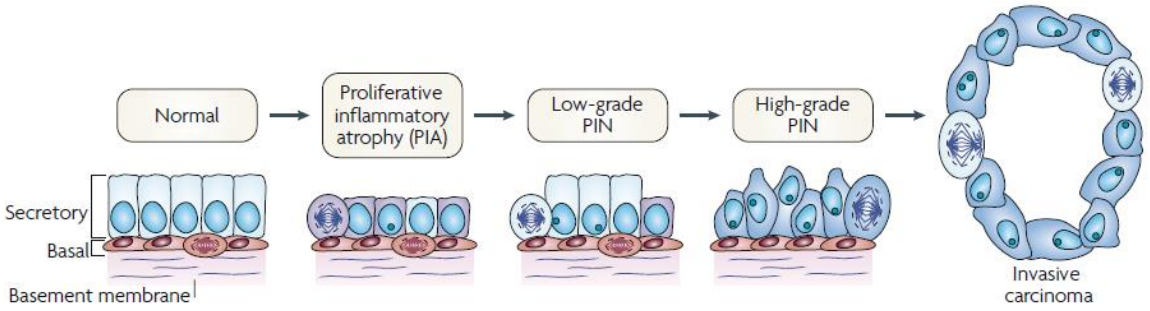

Figure 2. Cellular and molecular model of early prostate neoplasia progression. This stage is characterized by the infiltration of lymphocytes, macrophages and neutrophils. Phagocytes release reactive oxygen and nitrogen species causing DNA damage, cell injury and cell death, which initiate the beginning of epithelial cell regeneration. The downregulation of p27, phosphatase and tensin homologue (PTEN) and NKX3.1 in luminal cells stimulates cell-cycle progression. The proliferation of genetically unstable luminal cells and the further accumulation of genomic changes lead to progression towards invasive carcinomas (adapted from (35)).

As represented in Figure 2, PIN is the most likely pre-invasive stage of adenocarcinoma (36). PIN is characterized by cellular proliferation within pre-existing ducts and by cytologic changes mimicking cancer. PIN coexists with adenocarcinoma in more than 85% of cases but retains an intact or fragmented basal cell layer, unlike carcinoma, which lacks a basal cell layer, as seen in Figure 2 (37-38).

Concerning molecular pathways, PIN and PCA have low levels of cytoplasmic protein p27, which is a modulator of cell-cycle progression by inhibiting the activity of cyclin–dependent kinase complexes in the nucleus (39). The deletion of tumor suppressor genes such as Phosphatase and Tensin Homologue (PTEN) and NKX3.1 are also linked with PCa. The PTEN is responsible for the dephosphorylation and inactivation of PIP3, a second messenger required for the activation of the protein kinase AKT, wherein this activation is relevant for the inhibition of apoptosis (40). NKX3.1 is a prostate-restricted homeodomain protein that often contains single copy deletions in prostate cancer. In addition to suppressing the prostate cells growth, decreased NKX3.1 protein levels result in increased oxidative DNA damage (41). Highly ROS, like superoxide, hydrogen peroxide and nitric oxide are released from inflammatory cells and can damage DNA and interfere with cells division with unpaired or misrepaired damages, which results in cell death (42). Inflammatory cells also secrete cytokines that promote epithelial cell proliferation and stimulate angiogenesis (43). In terms of disease progression, inflammatory cells can migrate quickly through the extracellular matrix as a consequence of proteolytic enzymes release and their inherent mobile nature. Therefore, they might facilitate epithelial cell invasion into the stromal and vasculature compartments and, ultimately, support the tumor cells metastasis (44).

In addition to its role in physiological architecture and homeostasis of the prostate, androgens play an important role in PCa growth and survival, since they are main regulators of cell proliferation and control cell survival/death ratio (45). In advanced-stage prostate cancer, hormone therapy is no longer effective because cancerous cells have gained the ability to grow in the absence of androgens. At this stage most of the patients develop Androgen-independent Prostate Cancer (AIPC) (46).The most prominent player in AIPC progression is AR, a protein that binds androgens and acts as a transcription factor to regulate the transcription of a wide array of genes involved in various processes, including proliferation and growth (9).

The Figure 3 shows the progression of PCa, from the initial stage (androgen-dependent) until it becomes a more aggressive and lethal form (androgen-independent), through androgen ablation therapy. Firstly, multiple carcinogenic processes occur, whereby some cells are altered and begin to proliferate out of control. If the cancer is detected early, androgen ablation can be used for therapy via chemical castration or by surgical removal of the testicles, the main producers of androgens. This therapy is very effective in the destruction of androgen dependent cells. However, over time, this continuous androgen ablation results in the choice of cell subpopulations that can survive in the absence of androgens, leading to AIPC (9) (47).

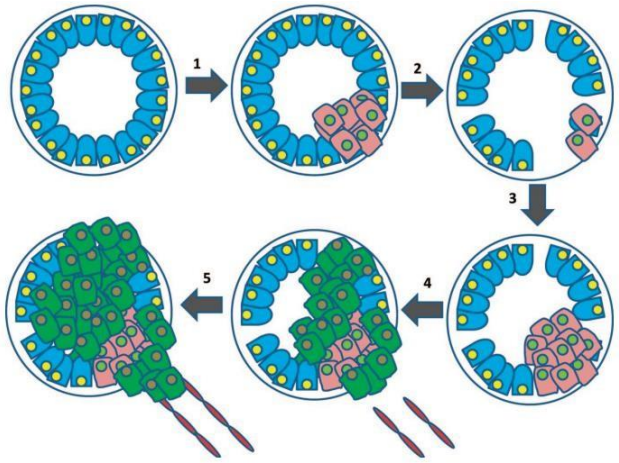

Figure 3. Progression from androgen-dependent to androgen-independent prostate cancers. 1. Various carcinogenic processes occur whereby some prostate cells proliferate out of control. 2. Prostate cancer cells are initially androgen dependent, and with androgen ablation therapy are successfully destroyed. 3. Some cells can survive to this treatment and continue proliferating. 4. Cells are now androgen independent and gain subsequent changes resulting in increased angiogenesis. 5. AIPC begins to metastasize to distant sites (adapted from (47)).

1.2.4 Diagnosis and Treatment

Early diagnostic of PCa is essential to further treatments, since generally patients only present symptoms in more advanced stages or metastatic stages of the disease (48). The main diagnostic tools include digital rectal examination, measurement of PSA serum concentrations and transrectal ultrasound-guided biopsies. PCa is detected by digital rectal examination in about 18% of all patients. PSA is a serine protease secreted by epithelial cells of the prostate and is the most well-known human prostatic secretory protein used as an indicator of PCa. However, as PSA levels above 3 ng/ml only indicate approximately 30% of risk of having PCa, it is necessary to combine it with other diagnosis methods as biopsies, allowing the elimination of false positives and false negatives of PSA tests (49).

The PCa treatment directly depends on the age of patient and state of the disease (50). If the tumor is small, local and has not spread beyond the gland, it is recommended a watchful waiting, defined by an active surveillance with PSA serum measurements and prostate biopsies (51). In pre-metastatic stages, the most common treatments include androgen-deprivation therapy, prostatectomy and brachytherapy. Hormonal therapy, radiotherapy and chemotherapy are applied in more aggressive and more advanced stages of PCa, and metastatic cancer (50). PSA is considered the most important biomarker for detecting, staging, and monitoring PCa in its early stage (29) (52-53). The main advantage of PSA testing is its superior sensitivity. The main disadvantage is that is not very specific since common pathological conditions such as BPH and prostatitis can also cause moderately to perceptibly abnormal test results. These false-positive results may lead to further diagnostic evaluation, increasing costs and use of more invasive procedures (54-57).

Many of these traditional forms of treatment are aggressive, invasive and diminish the patient's quality of life. Therefore, due to the limitations of the existing ones there is a need to discover and identify novel markers and therapeutic targets to improve the diagnostic and treatment minimizing the hazardous effects on patient health of existing methods.

1.2.5 Potential Biomarkers of Prostate Cancer

Nowadays, the identification of novel biomolecular markers and targets in PCa is critical for the development of improved diagnosis and therapeutic methods. Several proteins found overexpressed in PCa can act as potential biomarkers, but also can be considered immunotherapeutic targets, establishing new forms of treatment by targeting specifically cancer cells. These proteins show ability to modulate oncogenic functions through the cell surface (58-59).

In table 1 are summarized the description of other main biomarker for PCa and their respective functions.

Table 1. Description of main biomarkers for PCa and their respective functions.

Biomarker	Description	Function	References
PAP	Prostatic acid phosphatase	Role in prognostic intermediate and high-risk PCa. Distinguish poorly differentiated carcinomas. Reaction to androgen deprivation therapy of PCa that had metastasized.	(60-61)
PSMA	Type II integral membrane glycoprotein with enzymatic activities	High levels in primary PCa and metastatic disease, with presence of more than 90% of the protein in serum levels.	(62-64)
PSCA	Prostate cell surface-specific glycosyl phosphatidylinositol-anchored glycoprotein	Role in androgen-independent progression, metastasis or signal transduction. Expression associated with Gleason score, seminal vesicle invasion and capsular invasion.	(65-66)
AMACR	a-Methylacyl coenzyme A racemase	Growth promoter, independent of androgen in PCa. Enzyme greatly overexpressed in PCa High levels also in BPH	(67-69)
EPCA	Early prostate cancer antigen nuclear matrix protein	Early prostate cancer development Found in PCa precursor lesions, PIN and PIA.	(70-71)
GSTP1	Glutathione S-transferase P1	Gene hyper methylated in PCa. Acutely sensitive in PIN and PCa, distinguishing BPH.	(72-74)
GRN-A	Chromogranin A secretory acidic protein	Role in early neoplasic progression. Monitorization of PCa treatments. Prognoses AIPC.	(75-79)

In addition to the biomarkers described in Table 1, there are also a lot of biomolecules like Enhancer of zeste homolog gene 2 (EZH2), Urokinase plasminogen activator (uPA), Transmembrane protease serine 2 (TMPRSS2), Monocarboxylate transporters (MCTs), B7-H3, Caveolin-I, prostate cancer antigen 3 (PCA3), Golgi phosphoprotein 2 (GOLPH2) and DAB2 interacting protein (DAB2IP) that are able to be a PCa biomarkers. However, there is a need to wait for more studies to further evaluate and determine its effectiveness as a clinical PCa marker.

Finally, the Six-transmembrane Epithelial Antigen of Prostate 1 (STEAP1) is considered the most suitable candidate to be a potential therapeutic target, since show high serum levels associated with PCa cases (80).

2. Six-transmembrane Epithelial Antigen of Prostate Family

The STEAP protein family contains at least five homologous members. The STEAP family comprises STEAP1, STEAP2, STEAP3, and STEAP4. By the analysis of domain organization of STEAP family members (Figure 4), all proteins have in common a six-transmembrane domain, a COOH-terminal and an N-terminal. STEAP proteins uptake iron and copper because of two conserved histidine residues, where is predicted to bind at least an intramembrane heme group (81-82). The first role of STEAP protein was their contribution to metal homeostasis, through the reduction of iron and copper. Besides of contributing to metal homeostasis, STEAP family participates in maintenance of oxidative stress, cell-cell communication, proliferation and apoptosis. Nevertheless, the tissue-specific expression of STEAP family suggests they are assigned to distinct cellular functions and expression patterns (83). Indeed, STEAP3 seems to act as a potent metalloreductase essential for physiological iron absorption and STEAP4 appears to be rather involved in inflammatory stress, fatty acid and glucose metabolism (84). Finally, STEAP1, and in a lesser degree STEAP2, are highly overexpressed in different cancer types, but minimally expressed in normal tissues. Besides STEAP1, there is another related gene, STEAP1B, which may encode two different transcripts (STEAP1B1 and STEAP1B2) by post-transcriptional and post-translational mechanisms. Post-translational modifications (PTM) are intrinsically involved on regulating protein function and are crucial for a variety of cellular processes, such as transcription, replication, cell cycle, apoptosis and cell signaling (85). STEAP proteins possess important overlapping functions for growth and survival of cancer cells. Moreover, their subcellular localization diverges, since it is present either in plasma-membranous or in endosomal membranes. Due to their membrane localization and their high expression in many different cancers, including PCa, breast and bladder carcinoma and Ewing's sarcoma, STEAP proteins have been recognized and utilized as promising targets for cell- and antibody-based immunotherapy (84).

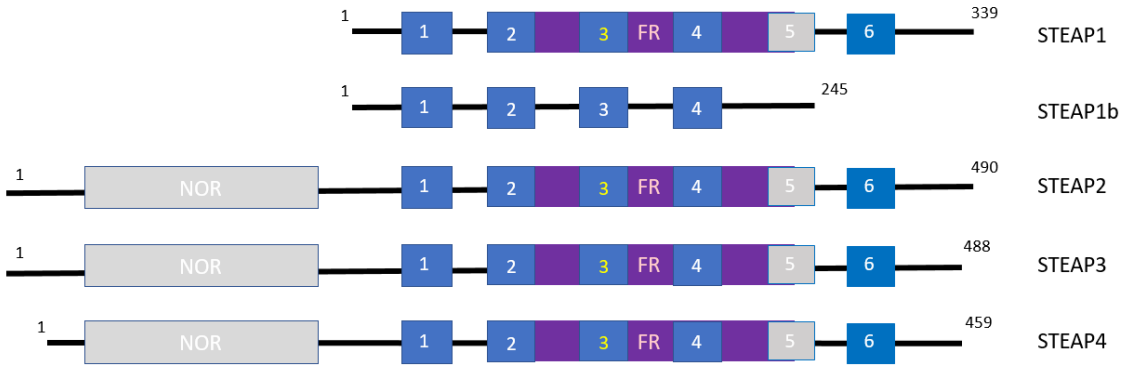

Figure 4. Schematic illustration of the domain organization of STEAP family. Superscript numbers indicate respectively the first and last amino acid. NOR: NADPH-oxidoreductase domain. The transmembrane domains are indicated as blue boxes. FR: ferric oxidoreductase domain. Heme-binding histidine residues within transmembrane domains 3 and 5 are indicated with orange lines (adapted from (84)).

2.1 STEAP1

2.1.1 Structure, Function and Expression

The STEAP1 protein was identified in 1999 by Hubert and coworkers as a novel marker and therapeutic target for PCa (89). The STEAP1 gene is located on chromosome 7q21.13, near of STEAP1b, STEAP2, STEAP3 and STEAP4, and comprises 10.4 kb, encompassing 5 exons and 4 introns. STEAP1 encodes a mRNA of 1.3 kb that is translated to a protein composed of 339 amino acids with a predicted molecular weight of 36 kDa. The protein contains 6-transmembrane domains with the COOH- and N-terminals located in the cytosol, and 3 extracellular and 2 intracellular loops (84) (86).

STEAP1 is mainly expressed in prostate epithelium, but high levels are also found in pericardium, peritoneum, fetal and adult liver, and human umbilical vein endothelial cells (83). Because of its localization on the cell membrane and its predicted 6-transmembrane domains, STEAP1 may presumably act as an ion channel or transporter protein in tight junctions and/or gap junctions, and thereby, it may be involved in cell adhesion and intercellular communication. As STEAP1 is overexpressed in cancer, it has been suggested that STEAP1 may facilitate cancer cell proliferation and invasion, perhaps through modulation of concentration of ions such as Na^+, K^+ and Ca^{2+} and small molecules (Figure 5). In addition, the modulation of K^+ and Ca^{2+} levels seems to be very important for the progression of prostate tumors toward androgen-independent stages, by conferring an apoptotic-resistant cellular phenotype (80) (82) (87). On the other hand, STEAP1 seems to facilitate cell growth by raising the intracellular level of ROS, showing that STEAP1 acts both on inter- and intracellular pathways (88). In addition, the fact that STEAP1 is found at endosomal membranes near to Transferrin Receptor 1 (TFR1) may possibly indicate its role in iron metabolism (83).

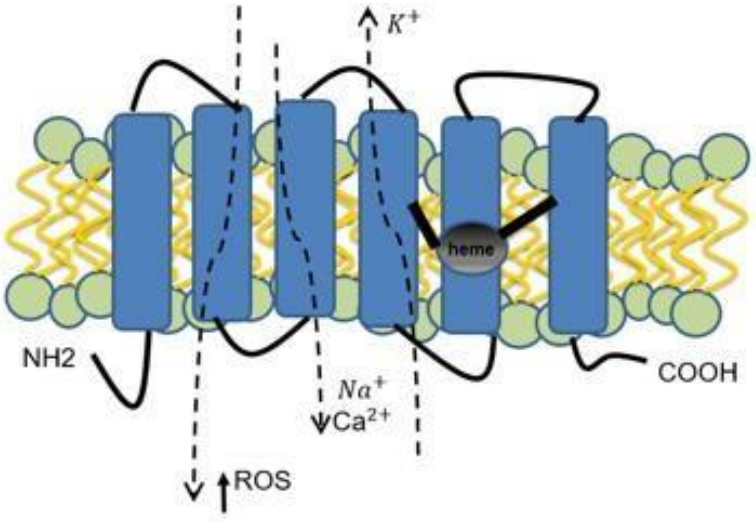

Figure 5. Schematic STEAP1 protein structure, cellular localization and physiologic functions. Presenting a six- transmembrane structure, intracellular COOH- and N-terminal, and intramembrane heme group. STEAP1 actively increases intra- and intercellular communication through the modulation of Na+, Ca2+ and K+ concentration, as well as the concentration of small molecules. It stimulates cancer cell proliferation and tumor invasiveness.

2.1.2 STEAP1 as a therapeutic target?

As previously mentioned, STEAP1 is highly expressed in PCa but also in other different types of cancer (86) (89). Thus, given its increased expression in cancer tissues, STEAP1 could be a promising target for immunotherapy. In immunotherapy, the immune system is manipulated to boost the natural defenses against tumor-associated antigens (TAAs), proteins that are overexpressed in cancer cells (90). In a successful immunotherapy, the vaccine must be capable of generating a tumor-specific T-cell responses to weakly immunogenic "self-antigens" (91).

In prostate cancers, STEAP1-specific Cytotoxic T Lymphocytes (CTLs) were found to inhibit the growth of transplantable prostate tumor cells in murine models (92-93). STEAP1 peptides have been recently demonstrated to induce antigen-specific CTLs able to recognize and destroy STEAP1-expressing tumor cells *in vitro* (93-94). Appropriate immunotherapy techniques require an increased expression or cross-presentation of self-peptides to naïve T-cells. Therefore, the ultimate purpose of tumor immunotherapy is the production of an effective $CD8^+$ and $CD4^+$ T-cell immune responses, leading to tumor regression. This vaccine should be administrated to patients with cancer without using invasive techniques (95). The application of an effective therapeutic vaccination based on STEAP1 is still at an early stage of development.

As a result, STEAP1 is see as a promising candidate biomarker to be imposed as a viable alternative for the therapeutics and diagnosis of PCa. So, the characterization of STEAP1 structure might allow the design of specific inhibitors that decrease and modulate its oncogenic function. However, high amounts of purified protein are required for structural, functional and interactions studies with potential drugs. For this it is necessary a sustainable biotechnological procedure that can deliver large amounts of proteins through a recombinant production of human

STEAP1 protein combined with a suitable chromatographic strategy.

3. Membrane Proteins

Membrane proteins may be classified according to their association with the membrane. The integral proteins that are embedded or cross the membrane are strongly associated through hydrophobic interactions. Integral proteins also contain more hydrophilic segments that contact with the cytosolic and exoplasmic sides of the membrane. The segments passing through the membrane may be composed of one or more α-helices or several ß-sheets. These proteins can only be extracted from the membrane with the use of organic solvents, denaturing agents or detergents, which interfere with hydrophobic interactions and disrupt the structure of the lipid bilayer (96). Integral membrane proteins can be solubilized with detergents (amphipathic molecules), which have a hydrophobic part that replaces membrane lipids and binds to protein hydrophobic portion, leaving the hydrophilic part of the detergent exposed to the aqueous medium (97).

Membrane proteins play a major role in many biological processes such as signaling, metabolism, solute and macro-molecular transport and bioenergetics. Thus, they are frequently pharmaceutical targets in many diseases. However, a deeper understanding of structure–function relationship of membrane proteins requires high-resolution structural information. To date, the Protein Data Bank (PDB) contains >26,000 structures, of which approximately 50% are annotated as distinct integral membrane proteins. Considering that 20%–25% of all proteins in a typical cell are integral membrane proteins, the number of known membrane protein structures represents a small fraction of all existing ones (98-99). The recombinant expression and subsequent purification of integral membrane proteins are already considered a major challenge but, combined with crystallization, they represent the biggest issue towards routine structure determination of membrane proteins (100). Consequently, the number of membrane proteins with known structure has remained negligible when compared to soluble proteins (101).

3.1 Solubilization of Membrane Proteins

Membrane proteins are naturally embedded in a mosaic lipid bilayer, which is a complex, heterogeneous and dynamic environment. This limits the use of many standard biophysical techniques to determine structure and function such as NMR, X-ray crystallography, circular dichroism, ligand-binding studies and, classical kinetic characterization. Such biophysical methods are impossible to conduct in the native environment since they require the protein extraction from its native membrane and solubilization in a detergent or lipid environment *in vitro* (102-103). Considering the complexities of the lipid bilayer, it is highly desirable to transfer membrane proteins to a more manageable environment for experimental studies. Such systems will consist of solubilizing components that must satisfy the hydrophobic nature of the

transmembrane segments, while loop regions stay into contact with an aqueous phase. The application of detergent micelles, mixed lipid/detergent micelles and liposomes are some of the systems applied in the reconstitution and crystallization of membrane proteins (102) (104-105).

Detergents are amphipathic molecules consisting of a polar head group and a hydrophobic chain. In aqueous solutions, they exhibit unique properties and spontaneously form spherical micellar structures. Membrane proteins are frequently soluble in micelles formed by amphiphilic detergents. Membrane proteins are solubilized by detergents creating a mimic of the natural lipid bilayer environment normally inhabited by the protein. They are usually crucial in protein isolation and purification (106).

Typically, membrane protein solubilization implies the use of detergents (96). Detergents are classified into four major categories according to their structure: ionic detergents, nonionic detergents, bile acid salts, and zwitterionic detergents. Figure 6 gives an example of each class of detergent.

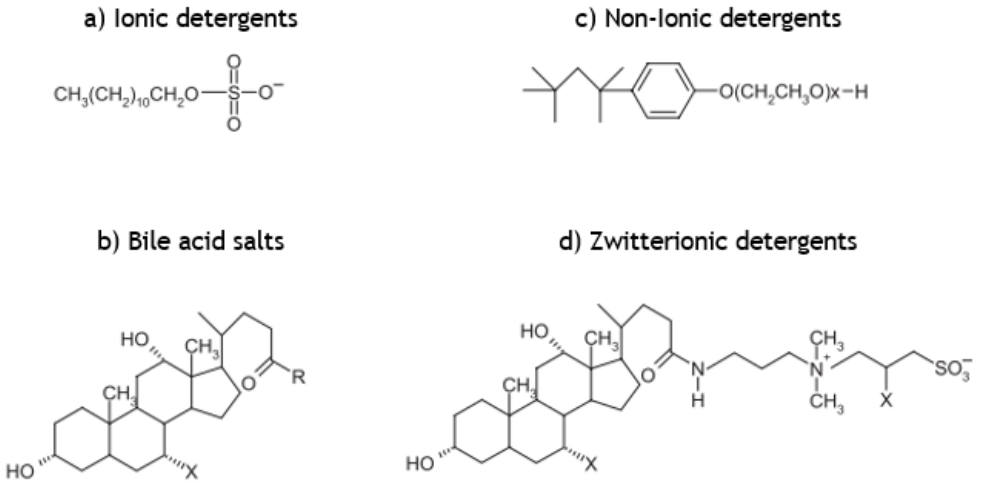

Figure 6. Structures of different types of detergents used in the solubilization of membrane proteins.

Ionic detergents contain a head group with a net charge that can be either cationic or anionic. They also contain a hydrophobic hydrocarbon chain or steroidal backbone. Ionic detergents, such as sodium dodecyl sulfate (SDS), are extremely effective in membrane proteins solubilization but are almost always denaturing (107). Bile acid salts are also ionic detergents but differ from SDS in their backbone, which consists of rigid steroidal groups. As a result, these bile acid salts have a polar and nonpolar face, instead of a well-defined head group, and they form small kidney-shaped aggregates. Bile acids are relatively mild detergents (108). Nonionic detergents contain uncharged hydrophilic head groups of either polyoxyethylene or glycosidic groups. They are generally considered to be mild and relatively non-denaturing. This allows many membrane proteins to be solubilized in nonionic detergents without affecting the protein's structural features (109). Finally, zwitterion detergents combine the properties of ionic and nonionic detergents and are in general more deactivating than nonionic detergents (109) (110).

3.2 Purification of Membrane Proteins

The protein purity is an essential pre-requisite for posterior structural and functional studies, like crystallization, or for therapeutic applications. Besides of requiring significant amounts and a high degree of purity, the protein must be in their active, stable and native conformation (111-113). In order to obtain these amounts, it is necessary the development of a suitable overexpression system, followed by a purification procedure. As a basic rule for any crystallization attempt, the protein should be chemically and conformationally homogeneous (99). The larger amount of protein produced, the higher chance of fulfilling these conditions. A larger quantity usually means a favorable protein/impurity ratio, and furthermore, it allows the isolation of only the purest fractions during purification (114).

Chromatography is the preferential separation technique, perhaps due to its high resolving power and the existence of several chromatographic strategies with different selectivity. There are various methods for the purification of biomolecules, however different types of chromatography have become dominant due to their resolution power. In contrast to other separation approaches that are limited to certain types of substances, chromatography can be applied to an extensive spectrum of compounds (115). The acceptance of chromatographic techniques can be attributed to their versatility. Each stationary phase has the ability to separate analytes by exploiting the affinity that each analyte has for the different ligands immobilized on the chromatographic support. On the other hand, the composition of the mobile phase, temperature and pH are main variables which can also be explored to purify the desired biomolecule (116). During the last years, several chromatographic techniques have been used for MPs purification, as single step or in combination with other techniques (117). The Immobilized metal-affinity chromatography (IMAC) is an affinity technique of chromatographic separation based in affinity between the immobilized metal ions on a solid matrix and the biomolecule in solution. This affinity results of reversible linkages formed between a metal ion chelated and certain groups in amino acids naturally presented or in residues of tags incorporated biotechnologically in target protein (118-119). These methods require often the addition of an affinity tag to protein during production step, which facilitates target protein binding to chromatographic matrix. Consequently, affinity tag removal is necessary after the purification step, which usually implies a significant reduction in process yield and irreversible activity losses. In addition, size exclusion chromatography or gel filtration is also applied to membrane proteins purification, in which fractionation is totally based on molecular size. The size exclusion chromatography (SEC) is considered appropriate for a final purification step, such as polishing and final desalting in a downstream bioprocess. This technique has the main gain that can be employed for purification of any kind of protein and permitted that target protein retains its bioactivity since no molecular interactions are established. Nevertheless, resolution is very low, and is not able to distinguish proteins with small differences in their molecular weight (120-121). Ion-exchange chromatography (IEC) is a suitable separation technique often used in early stages of purification. The biomolecules are separated based on electrostatic interactions between protein and the charged ligands, cation or anion exchangers (122). Thus,

there are two types of IEC: a cation exchange chromatography where anion exchangers interact to positive charged molecules and anion exchange chromatography where cation exchangers bind anionic molecules (123). Generally, compounds of the load sample are retained at low salt concentrations and the elution can be achieved by increasing the ionic strength or by changing pH. The many advantages of this method are the support low cost, high flow rates that allows large-scale trials and the well described protein-matrix interactions and binding/elution conditions. However, detergents must be used with some careful during protein purification by IEC, since ionic detergents might interfere with the ionic chromatographic performance step (122) (124).

HIC is nowadays established as a powerful bio separation technique, both on a laboratory scale and on an industrial scale, for the purification of biomolecules (115) (125-126).

3.2.1 Hydrophobic Interaction Chromatography

The Hydrophobic Interaction Chromatography is one of the classical preparative chromatography method and it has been successfully used for the isolation of therapeutic biomolecules, including proteins (125) (127-131) and DNA plasmids (132-134). HIC promotes the separation of biomolecules based on the interaction between hydrophobic ligands immobilized on the support and non-polar regions of biomolecules that are exposed on surface at higher concentrations of salt, especially antichaotropic salt (115). In HIC, as shown in Figure 7, biomolecules retention is promoted with high concentrations of salt in the mobile phase, being the elution generally promoted by simply decreasing the ionic strength of buffer and/or by adding organic solvents or some detergents. The mobile phase properties (salt type, ionic strength, pH), the stationary phase characteristics (matrix chemical nature, type of hydrophobic ligand, chain length and degree of ligand substitution) and temperature are factors that generally affect the chromatographic behavior of biomolecules in HIC type (135-136).

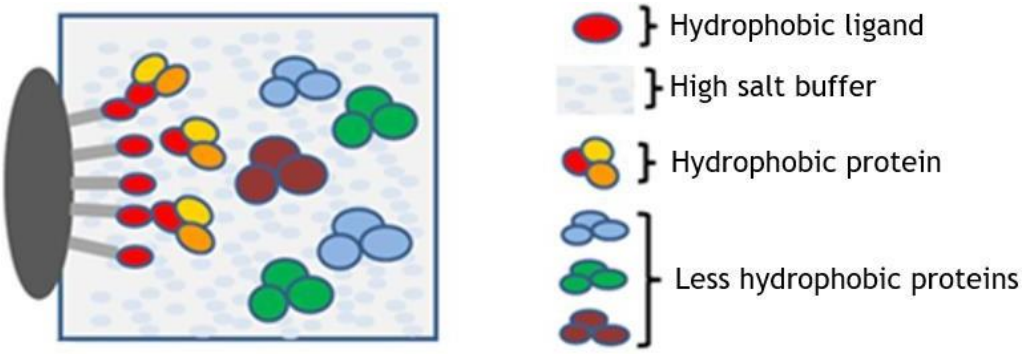

Figure 7. Mechanism of adsorption of biomolecules on hydrophobic interaction chromatography. Biomolecules of interest, with strong hydrophobic characteristics, interact with the ligand, while the ones with low hydrophobicity do not bind and are removed in the flow-through.

This type of interaction appears when non-polar compounds are placed into water. In this

situation, an increase in entropy is observed (ΔS>0), resulting from a displacement of the ordered water molecules around the non-associated hydrophobic groups to free bulk water (137). Employing this chromatographic technique, the protein structural alterations are minimal, since the forces involved are relatively weak (Van der Walls forces), which allow the maintaining of their biological activity, (118). Hydrophobic interactions are the most important noncovalent forces responsible for protein structure stabilization, binding of enzymes to substrates and protein folding (138-139)

The effect of salt type on protein retention has been shown to follow the Hofmeister series (Figure 8) for the precipitation of proteins in aqueous solutions (140). Antichaotropic salts, at the begin of the series, has higher polarity and bind water strongly, which induces exclusion of water on the protein and ligand surface, promoting hydrophobic interactions and/or protein precipitation (salting-out effect). Additionally, the presence of this type of salts has a stabilizing effect on protein structure. In contrast, chaotropic salts, at the end of the series, have less polarity and bind water loosely, which induces inclusion of water on the protein and ligand surface, and thus tend to decrease the strength of hydrophobic interactions (salting-in effect) (141).

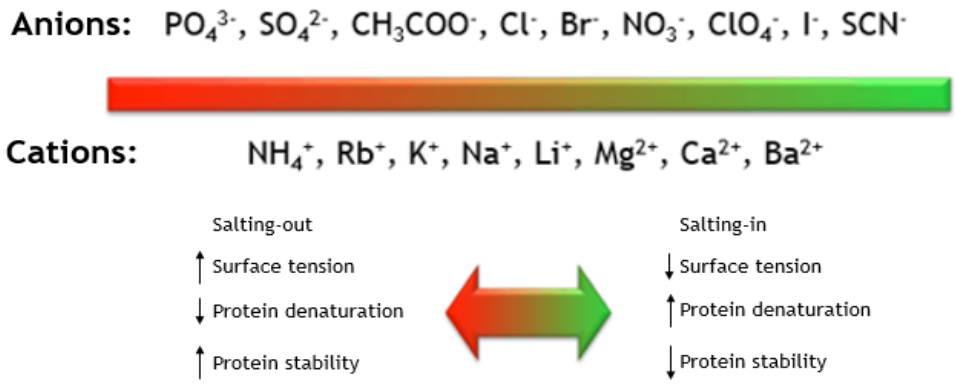

Figure 8. Hofmeister series and effects of some anions and cations on proteins (adapted from (140)).

Proper selection of salt type in the eluent results in significant changes not only in the retention of the total protein, but also in the selectivity of the separation (142-143). Different authors have shown that selectivity changes when different types of salt are applied in the mobile phase (144-145). For neutral and cosmotropic salts, such as ammonium sulfate and sodium chloride, protein retention increases with increasing salt concentration (141). Ligands with an intermediate hydrophobic character are more efficient than ligands that promote strong hydrophobic interactions, since they apply moderate forces and the elution of biomolecules can be achieved by a simple decrease of salt concentration, avoiding the use of organic solvents or detergents (115). The most commonly used ligands in HIC are straight chain alkanes (such as Butyl, Octyl) and some aromatic groups (such as phenyl) as demonstrated in figure 9.

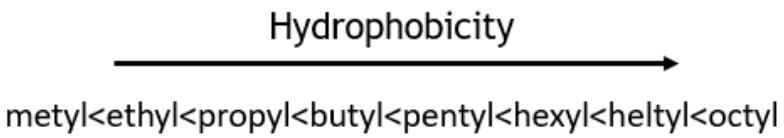

Figure 9. Hydrophobicity scale of n-alkane ligands (115)

With increasing length of the n-alkyl chain there is an increase in hydrophobicity and strength of the interaction between the protein and the matrix, but the selectivity of the adsorption can decrease. In opposition, an increase in the degree of substitution of the support leads to an increase in the binding capacity of the stationary phase, due to the high chance of multi-point bonds formation leading to denaturation due to the use of harsh conditions in protein elution (143).

Indeed, HIC appears to be an excellent approach for membrane protein purification since exploits the hydrophobic properties on a more polar and less denaturing environment than RPC, in which there is an application of non-polar solvents for protein elution. Furthermore, biomolecules damage is smallest than on IMAC, SEC, IEC or RPC due to the weakly interactions such Van der Waals forces accountable for membrane proteins support onto cell membrane. These forces are also the main reason for hydrophobic interactions and in conjunction with application of mild conditions, to keep biological activity of proteins in HIC (115).

Chapter 2

Aims

Currently, STEAP1 is a promising candidate biomarker to be imposed as an alternative therapeutic and diagnosis target, due its overexpression and potential role in PCa. Thereupon, the resolution of its 3D structure and the further functional and biointeraction studies may shed some light on the actual role of STEAP1 in PCa. For this, the development of sustainable biotechnological procedure is required to obtain enough quantities of highly pure STEAP1.

The main aim of this master thesis was to develop a one-step chromatographic strategy for the purification of STEAP1, recovered from *Pichia pastoris* lysates, using hydrophobic interaction chromatography. In order to achieve this objective, two intermediate goals were define to:

- Improve the recovery yield of STEAP1 from *Pichia pastoris* lysates by establishing the most effective detergent for the solubilization of the target protein.
- Develop a hydrophobic interaction isolation procedure by evaluate the performance of Octyl- and Butyl-Sepharose according to the conditions required for the binding and elution of STEAP1 on these matrices.

Chapter 3

Materials and Methods

1. Materials

Ultrapure reagent-grade water was obtained from a Milli-Q system (Millipore/Waters). Calcium chloride dihydrate, dithiothreitol (DTT), sulfuric acid (H_2SO_4), SDS and Phenylmethylsulphonyl fluoride (PMSF) were obtained from PancReac AppliChem (Darmstadt, Germany). Zeocin™ was purchased from InvivoGen (Toulouse, France). Deoxyribonuclease I (DNase), glass beads (500 µm) and proline were obtained from Sigma-Aldrich Co. (St Louis, MO, USA). Yeast nitrogen base (YNB) was obtained Pronadisa (Malaysia). Yeast extract and glycerol were acquired from HiMedia Laboratories (Mumbai, India). Glacial acetic acid and potassium hydroxide were obtained from CHEM-LAB N.V (Zedelgem). CHAPS were obtained from Fisher scientific (Epson, United Kingdom). Agar, ammonium hydroxide, glucose, hydrochloric acid, tris-base, methanol, dimethyl sulfoxide, phosphoric acid, Tween-20, bovine serum albumin (BSA) were obtained from Thermo Fisher Scientific UK (Loughborough, UK). Biotin was obtained from Roche (Basileia, Swiss). The NZYColour protein marker II was purchased from NZYTech (Lisbon, Portugal). Antifoam A was obtained from Sigma-Aldrich (St. Louis, MO, USA), Bis-Acrylamide 30% was obtained from Grisp Research Solutions (Porto, Portugal). All other chemicals were of analytical grade commercial available and used without further purification.

2. Methods

2.1. Strain, plasmids, and media

The plasmid pICZαB-STEAP1_His6 (Invitrogen Corporation, Carlsbad, CA, USA) was previously produced by our research group and used for recombinant STEAP1 production into *Pichia pastoris* X33 Mut^+ strain (from Invitrogen, EasySelect™ *Pichia* Expression Kit no. 25, 2010). The *Pichia pastoris* transformants were selected on YPD plates (1% yeast extract, 2% peptone, 2% glucose and 2% Agar) supplemented with 200 µg/mL Zeocin™.

Pre-fermentation process was carried out in BMGH medium (2% YNB, 4x10-4 g/L biotin and 1% glycerol, 1 M potassium phosphate buffer pH 6.0) supplemented with 200 µg/mL Zeocin™. The bioreactor fermentation was performed in BSM medium (20.3 mL/L H_3PO_4, 0.5g/L $CaCl_2$, 11.3 g/L $MgSO_4.7H_2O$, 3.1 g/L KOH, 40 g/L Glycerol), supplemented with a trace elements solution, SMT (27 g/L $FeCl_3 \cdot 6H_2O$, 2 g/L $ZnCl_2$, 2 g/L $CoCl_2 \cdot 6H_2O$, 2 g/L $Na_2MoO_4 \cdot 2H_2O$, 1 g/L $CaCl_2 \cdot 2H_2O$, 1.2 g/L $CuSO_4$ and 0.5 g/L H_3BO_4, prepared in 1.2 M HCl) and 250 µg/mL Zeocin™.

2.2 STEAP1 Biosynthesis

Pichia pastoris X33 Mut$^+$ transformed with the vector pPICZαB-STEAP1_6His was streaked and selected on YPD plates, growing at 30ºC. Then, a single colony was picked and transferred to 100 mL of BMGH medium and grown overnight at 30ºC and 250 rpm until the optical density at 600 nm (OD600nm) typically reached 5-6. The inoculation volume to be collected from the pre-cultivation was calculated to fix the initial OD_{600nm} at 0.5. The batch and fed-batch processes were carried out in 750 mL bench-top parallel mini-bioreactors (Infors HT, Switzerland) with 250 mL of BSM medium previously sterilized and supplemented with Zeocin™ and an SMT solution. The pH and temperature were kept constant throughout the batch and fed-batch mode, respectively at 4.7 and 30ºC. The pH was controlled by the automatic addition of 0.75 M H_2SO_4 and 12.5 % (v/v) NH_4OH through two peristaltic pumps. The methanol and glycerol feeding profiles applied were maintained and controlled by automated peristaltic pumps controlled through the IRIS software. Briefly, the fermentation process implemented by our research group for recombinant STEAP1 biosynthesis into *Pichia pastoris* bioreactor cultures have three main stages: the glycerol-batch, the fed-batch and methanol induction phase. The pellets were obtained from *P. pastoris* mini-bioreactor culture with a glycerol batch-phase (20 hours), a 50% (v/v) gradient glycerol feed followed by a 100% (v/v) methanol constant feeding during 10 hours, supplemented with 6 % (v/v) DMSO and 1M Proline (146).

2.3 Cell lysis and STEAP1 solubilization

The protocols for *Pichia pastoris* lysis and protein recovery were previously optimized by our research group (146). Briefly, the cells were harvested by centrifugation for 5 minutes at 1500g, 4ºC and stored frozen at -20ºC until the samples were used. Prior to the cell lysis, a centrifugation was performed at 1500g for 10 minutes at 4ºC. The cell lysis, it was performed by a combination of a mechanical and physical lysis, based on vortex-ice cycles. The *Pichia pastoris* suspensions were lysed with a lysis buffer (50 mM Tris Base, 150 mM NaCl, 10 mM DTT, 1mM $MgCl_2$, pH 8.0), protease inhibitors (1 mM PMSF) and glass beads. The mixture was carried out in the proportion of 1:2:2 (for 1 g biomass, 2 g glass beads, and 2 mL lysis buffer). It was vortexed 7 times for 1 minute with an interval of 1 minute on ice. For the removal of cell debris, a new centrifugation was done at 500g, for 5 minutes at 4ºC. A portion of lysis buffer was further added to improve the elimination of cells debris and glass beads. Subsequently, the supernatant was collected to a lysis tube, DNase (1 mg/mL) was added, and it was centrifugated at 16000g for 30 minutes at 4ºC. The pellet was resuspended in a solubilization buffer (lysis buffer plus 1% (v/v) Triton X-100, pH 7.8) at 4ºC until full solubilization nearly 10-12 hours. The protein content on the lysate was then quantified before injected on ÄKTA™ Avant and the samples were frozen at -20ºC for further analysis.

2.4 Total protein quantification

The total protein quantification in the lysates obtained after solubilization was quantified by Pierce BSA Protein Assay Kit (Thermo Fisher Scientific, Waltham, MA, USA). The use of BSA was required as standard, according to manufacturer instructions. Briefly, 10 µL of each sample, blank or standard (in triplicates) and 200 µL of Working Reagent (Reagent A and B were provided by the manufacturer) were added to each well and homogenized. The plate was then incubated at 37°C for 30 minutes (dark conditions). The 96 well plate was read in a xMark™ Microplate Absorbance Spectrophotometer (Bio-Rad) at 562 nm.

For the calibration curves, several solutions of different BSA concentrations (ranged between 25-2000 µg/mL) were prepared in triplicates using the protein solubilization buffer (50 mM Tris Base, 150 mM NaCl,10 mM DTT, 1mM $MgCl_2$, pH 7.8) and a dilution degree of 1:10, depending on sample concentration, was required. The following calibration curve was used to quantify all the cell lysates:

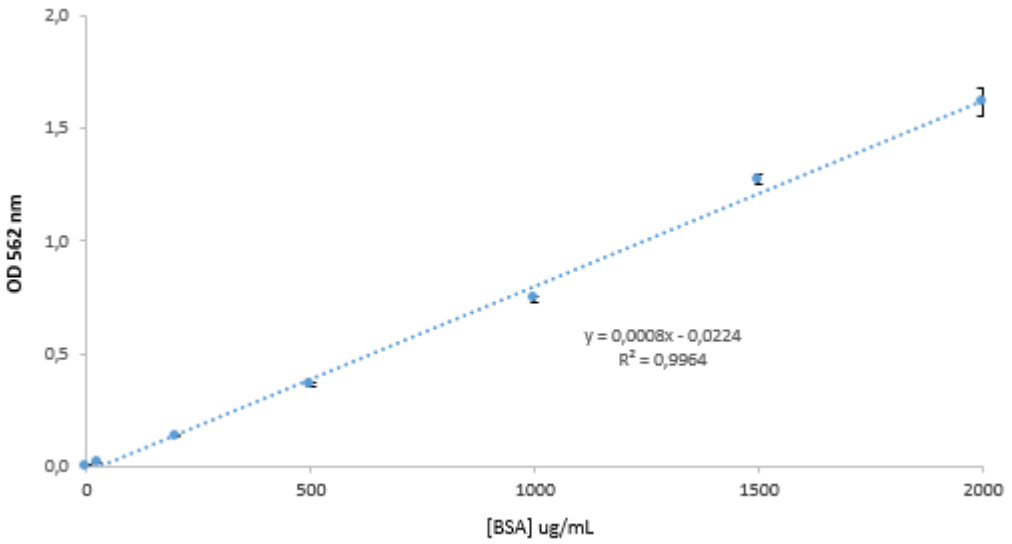

Figure 10. BSA calibration curve for total protein quantification (µg/mL) ranged between 25-2000 µg/mL.

2.5 STEAP1 purification by Hydrophobic Interaction Chromatography

The chromatographic assays were performed at room temperature in an ÄKTA Avant system with UNICORN 6 software (GE Healthcare, Uppsala, Sweden) equipped with a 500 µL injection loop. All buffers pumped in the system were prepared with Mili-Q system water, filtered through a 0.20 µm pore size membrane (Schleicher Schuell, Dassel, Germany) and degassed ultrasonically. The HIC stationary phases understudy, Butyl-Sepharose 4FF and Octyl-Sepharose 6FF, were purchased on GE Healthcare Biosciences. Both hydrophobic media were packed according to company guide-lines (10 mL of gel volume) into a XK16 glass column purchased from GE Healthcare Biosciences. Screening experiments were performed using different resin combinations and salt concentrations in order to determine the best salt concentration required for the retention of STEAP1 in each

stationary phase. Unless otherwise stated, the stationary phase's Octyl- and Butyl-Sepharose were equilibrated with 600 mM, 750 mM, 800 mM and 1000 mM sodium phosphate buffer and monosodium phosphate with sodium chloride (pH 8.0) at a flow rate of 1 mL/min. The solubilized pellet containing STEAP1 (1 mL with a protein concentration near 10.4 mg/mL) were injected onto the column using a 500 µL loop at the same flow rate and salt concentration. After elution of unretained species at the salt step, ionic strength of the buffer was decreased to 50 mM phosphate buffer (pH 8.0). This condition was maintained with 3 column volume (CV) in order to elute the bound and weakly retained species. Subsequently, the strongly bound species were eluted by a linear and step detergent gradient from zero to 1% of Triton X-100 in 50 mM sodium phosphate buffer, with 3 CV. Finally, a wash step was applied with 1% Triton in 50 mM phosphate buffer with 1 CV. In all the chromatographic runs, absorbance and conductivity was continuously monitored at 280 nm and 1.8 mL fractions were collected. Subsequently, the fractions were pooled according to the chromatograms profile obtained, concentrated and desalted with Macrosep® Advance centrifugal devices with Omega™ membrane (VWR) and conserved at 4ºC for further analysis.

2.6 SDS-PAGE and Western Blotting

Reducing Sodium Dodecyl Sulphate-Polyacrylamide Gel Electrophoresis (SDS-PAGE) and western blot trials were performed, respectively according to the method of Laemmli. SDS-PAGE samples were prepared in a loading buffer (500 mM Tris-Cl (pH 6.8), 10% (w/v) SDS, 0.02% (w/v) bromophenol blue, 0.2% (v/v) glycerol, 0.02% (v/v) 2-mercaptoethanol) at a ratio of 3:1 (15 µL of sample to 5 µL of loading buffer), denatured at 100ºC for 15 minutes and were run on 4% stacking and 12.5% resolving gels at 120V during approximately 2 hours at room temperature with a running buffer (25 mM Tris, 192 mM glycine and 0.1% (w/v) SDS). After electrophoresis, one gel was stained by Coomassie brilliant blue and the other gel was transferred to a polyvinylidene difluoride (PVDF) membrane 6x9cm (GE Healthcare, Buckinghamshire, UK,) in order to perform the western blots experiments. Proteins were transferred over a 45 min period at 750 mA at 4ºC in an electrotransfer buffer (25 mM Tris, 192 mM glycine, 10% (v/v) methanol and 10% (v/v) SDS). After the blotting, the membranes were blocked with TBS-T (pH 7.4) containing 5% (w/v) non-fat milk for 60 min at room temperature, washed 3 times for 15 minutes each and incubated overnight with a rabbit polyclonal antibody against human STEAP1 (sc-271872, diluted at 1:100 Santa Cruz Biotechnology, Dallas, Texas, U.S.A.) at 4ºC with a constant stirring. Then, the membranes were washed 3 times for 15 min each with TBS-T and adherent antibody was detected by incubation with an anti-rabbit (NIF 1317, diluted 1:20000; Santa Cruz Biotechnology, Dallas, Texas, U.S.A) for 1 hour at room temperature with constant stirring. Finally, PVDF membranes were washed again, exposed to 700 mL ECL substrate (Biorad, Hercules, USA) for 5 minutes and visualized on the Molecular Imager FX (Biorad, Hercules, USA). In alternative, we used a dot blot protocol with application of 20 µL of samples onto a PVDF membrane previously activated with pure methanol and equilibrated with Mili-Q water and TBS. Then, we let the membrane dry before blocking non-specific sites by soaking

in 5 % (w/v) non-fat milk in TBS-T during 60 min. After the blocking step, the membranes were incubated with the same primary and secondary antibodies applied for Western blotting. Membrane's analysis follows the same final steps as stated above for Western Blotting.

Chapter 4
Results and Discussion

1. STEAP1 solubilization

As referred previously, a suitable isolation procedure for further structural, functional and biointeraction studies has a main importance to obtain a complete characterization of membrane proteins in order to understand the 3D-native structure and then generate drugs that target specific sites inside the protein.

Researchers in the field indicate the difficulties in handling membrane proteins due its problematic experimental behavior, since extraction of membrane proteins from the phospholipid bilayer environment is a critical first step in their purification and structural characterization. This extraction requires disruption of the bilayer structure to promote protein removal, without also irreversibly disrupting the protein structure. The primary agents used to extract membrane proteins are amphiphilic molecules such as detergents that can substitute for and mimic the stabilizing properties of the natural phospholipids (105) (147-149). This fact leads to the expectation that these proteins are dramatically harder to produce than soluble proteins. One of the reasons may be the inadequate use of detergents during extraction and purification. Therefore, it was crucial to choose the right detergent for an efficient extraction and purification of the membrane protein of interest (106-107).

Although *Pichia pastoris* X33 are able to secrete heterologous proteins to extracellular medium, it was necessary recover STEAP1 by disruption the host cell wall, applying *Pichia pastoris* lysis with glass beads. This technique is considered the simplest and the most appropriate for lab-scale cell disruption, since it can preserve the stability of the target protein (150-151). This procedure was optimized for hMBCOMT by our research team (146) and consists in vortexing cells, shared with lysis buffer and glass beads, for 7 cycles of 1 min with an interval of 1 min on ice. Protease inhibitor (PMSF) and DNase were also used to prevent protein degradation and digest nucleic acids respectively.

So, the effect of different detergents at 1% (v/v) were evaluated to determine the most appropriate to STEAP solubilization, including one ionic (SDS), four non-ionic (Tween-20, Tween-80, NP-40 and Triton X-100) and one zwitterionic (CHAPS). As reported in Figure 11, by western blot analysis, the pellet solubilized with only lysis buffer did not show any immunodetection, proving that detergents are really necessary to stabilize the target protein in a correct native molecular weight (147). SDS, Tween-20, Tween-80, CHAPS and NP-40 showed weak STEAP1 solubilization and thus were not considered efficient in this step. Finally, Triton X-100 achieved the most promising results, preserving STEAP1 native structure with the highest expression patterns in comparison with other samples. This can be explained by the fact of some membrane

proteins are soluble only in a single detergent species that fulfills specific solubilization requirements, while others are soluble in many different detergents but are only functionally active in one of them (106).

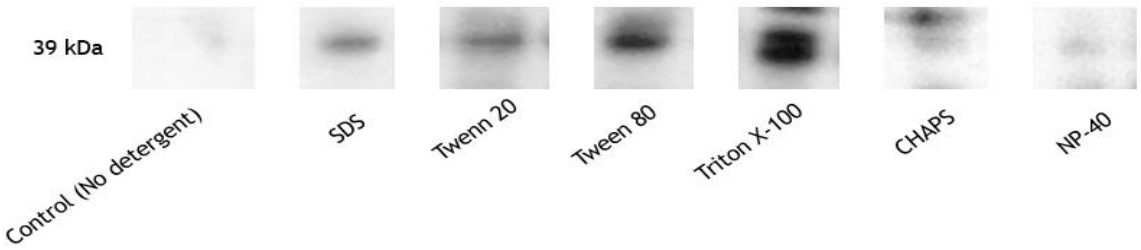

Figure 11. Western blot analysis of the STEAP1 solubilization using 1% (v/v) of some common detergents applied in the literature.

2. Purification screening trials onto Octyl-Sepharose

During the last years, HIC has been developed by many researchers and today is an established and powerful bioseparation technique in laboratory-scale purification of biopharmaceuticals, although successful applications of HIC in the purification of integral membrane proteins are unusual (115). However, there are several studies applying hydrophobic adsorbents successfully by our research group, such as Human Soluble Catechol-*O*-methyltransferase (hSCOMT) (152) and Human Membrane Bound Catechol-*O*-methyltransferase (hMBCOMT) (153). Nevertheless, due to strong hydrophobic character of STEAP1, mainly provided by its membrane anchor region, HIC can be seen as a suitable method for its isolation. In HIC, hydrophobicity of resins affects mainly protein retention. The larger the n-alkyl chain length, such as verified in Octyl-Sepharose, the highest matrix hydrophobicity. Figure 12 show the resin structure of adsorbents studied in this work.

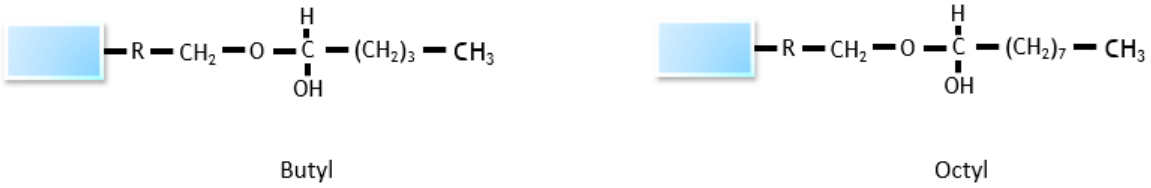

Figure 12. Schematic structures of Butyl- an Octyl-Sepharose ligands (adapted from (115)).

Therefore, we intend for the first time to understand the application of two commercial hydrophobic adsorbents (Octyl- and Butyl-Sepharose) in terms of retention and elution conditions for STEAP1, in order to design an appropriate downstream procedure.

Generally, for membrane proteins purification by HIC is required the choice of a suitable salt, detergent and the assortment of the most appropriate parameters for protein stability. Mahn and coworkers recommended the use of sodium chloride, sodium citrate, ammonium sulfate and sodium phosphate in HIC (154).

Consequently, in initial trials we pretended understand the effects of mild concentrations of different salts on STEAP1 retention onto the Octyl adsorbent, since additional studies by our research group (152-153) demonstrated that the recovery of a membrane protein is allowed with mild elution conditions. As represented in table 2 and figure 13 these initial trials consisted in a sample loading at 500 mM of monosodium phosphate, disodium phosphate, sodium phosphate buffer, sodium chloride, sodium citrate and ammonium sulfate followed by a decreasing ionic strength gradient with 50 mM of sodium phosphate buffer.

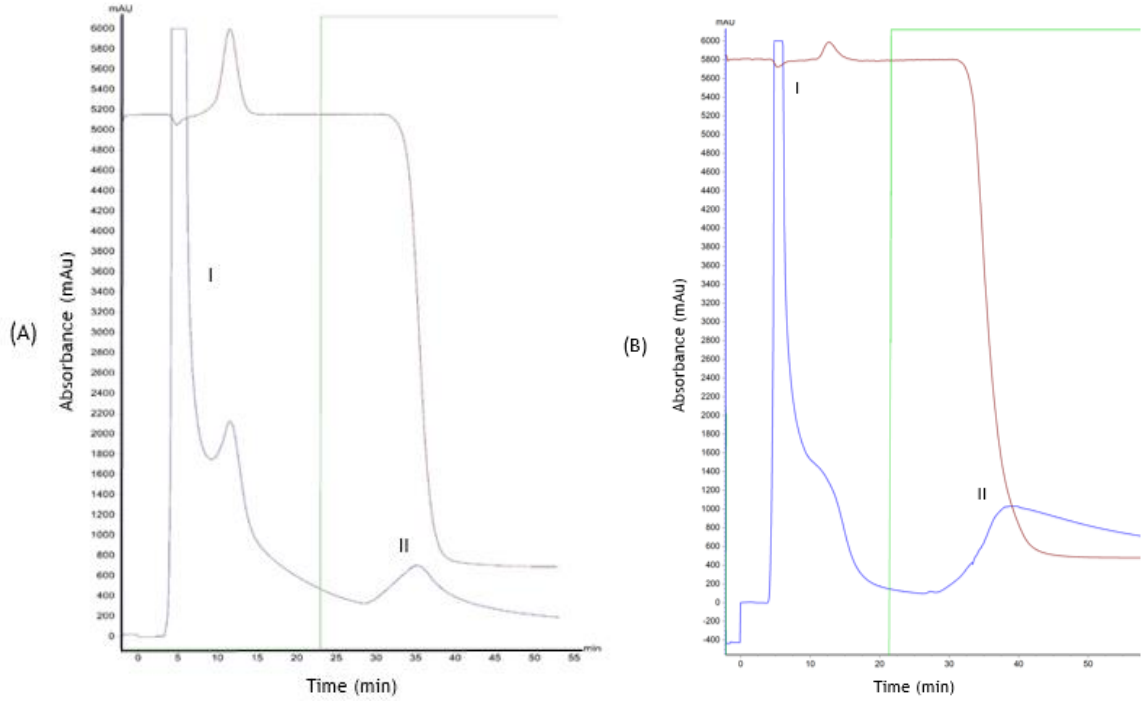

Figure 13. Initial purification screening trials on Octyl-Sepharose. (A) sodium chloride; (B) sodium phosphate buffer. Adsorption was performed at salt concentrations of 500mM (pH 8.0). Desorption was performed with 50 mM sodium phosphate buffer (pH 8.0). Different color lines represent the absorbance at 280 nm, brown line the conductivity and the continuous green line represents sodium phosphate buffer concentration.

Table 2. Summary of salts concentrations used in isolation screening trials and STEAP1 elution behavior onto an Octyl-Sepharose support.

	Several Salts [500mM]	STEAP1 Retention	STEAP1 Elution Behaviour
			Sodium Phosphate Buffer (50 mM)
Chromatographic methodologies	Monosodium phosphate	-	-
	Disodium phosphate	-	-
	Sodium phosphate buffer	+	+
	Sodium chloride	-	+
	Sodium citrate	---	
	Ammonium sulfate	-	

(−) to (+) denotes respectively no retention/retention and no elution/elution of STEAP1 on Octyl-Sepharose

The screening of chromatographic profiles showed in Figure 13 by Dot blot (Figure 14), SDS-PAGE and Western Blot analysis (Figure 15) demonstrated that with mild concentrations such 500mM of monosodium phosphate, disodium phosphate and ammonium sulfate there are any STEAP1 adsorption onto the support. So, the first three salts will no longer be evaluated. In contrast, with sodium chloride and sodium phosphate buffer, is promoted an incomplete STEAP1 retention on Octyl-adsorbent. The higher molecular weight contaminants are eliminated in peak I and II [figure 15(A)] with 500 mM of salt while the protein of interest is retained on matrix and partially eluted in peak II as judge by the confirmation of immunological active strong band onto Western blot [Figure 15(B)]. So, a low level of contaminants is likely to be eluted with the target protein. Using sodium citrate there is a strong STEAP1 signal in peak I which indicates no STEAP1 retention onto the adsorbent, being directly eluted. This could indicate the future application of one negative chromatography approach.

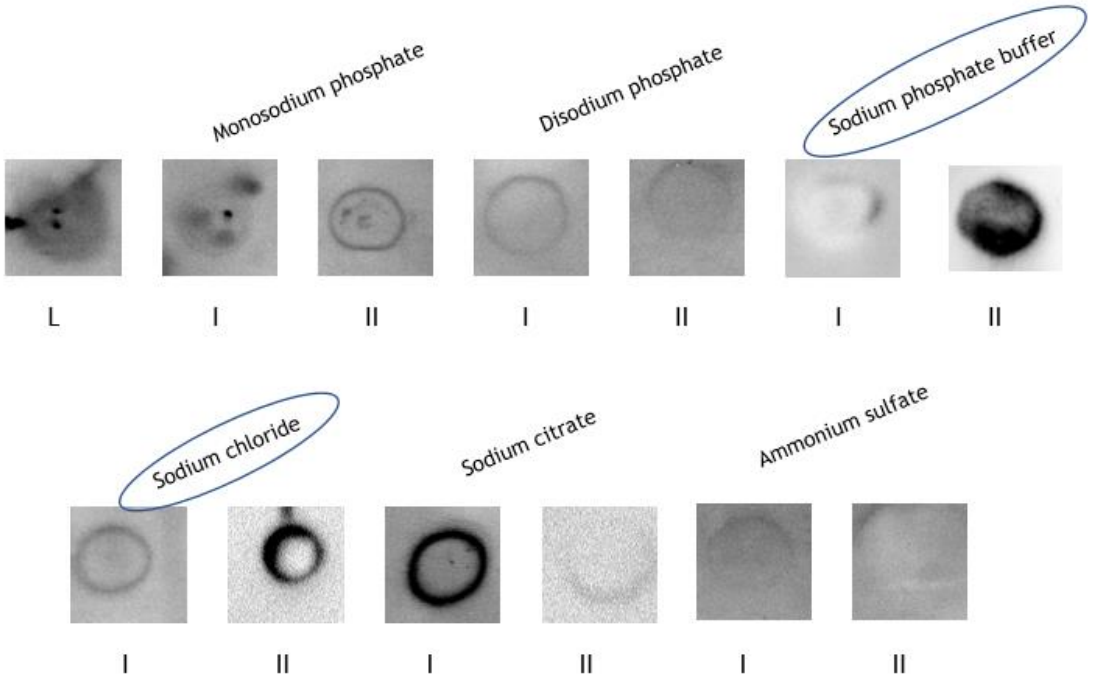

Figure 14. Dot blot analysis of samples collected on chromatographic profiles of figure 13. L – solubilized lysis pellet; Lane I – Peaks I obtained at 500 mM of sodium chloride and sodium phosphate buffer on Octyl- and Lane II – Peak II obtained with 50mM sodium phosphate buffer on Octyl-Sepharose.

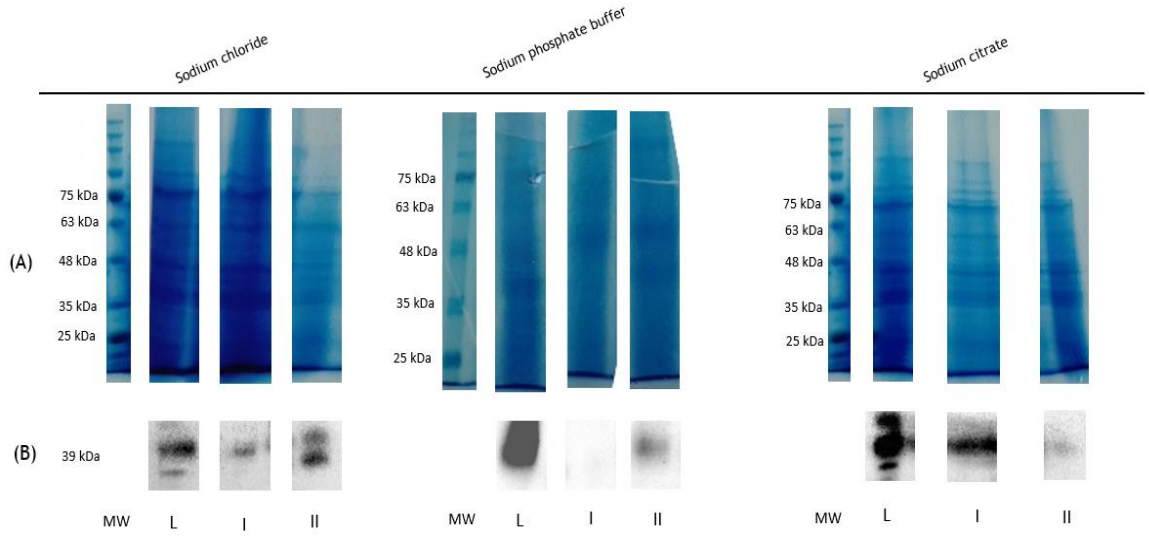

Figure 15. SDS-PAGE (A) and Western blot (B) analysis of samples collected on chromatographic profiles of figure 14. L – solubilized lysis pellet; Lane I – Peaks I obtained at 500 mM of sodium chloride and sodium phosphate buffer on Octyl- and Lane II – Peak II obtained with 50mM sodium phosphate buffer on Octyl-Sepharose.

Although the occurrence of STEAP1 expression in *Pichia pastoris* lysates extracts (Figure 15), there is no complete STEAP1 adsorption on the hydrophobic support, which can be explained by low ionic strength in mobile phase that is not enough to promote total retention. This behavior can be explained due highly hydrophobic resin such Octyl-Sepharose resulting in higher length in the alkyl chain and consequently stronger interactions established between STEAP1 and matrix.

Usually, when strong interactions are established between the target protein and hydrophobic supports the use of organic solvents, detergents and chaotropic agents that are aggressive elution's agents can be applied (115). Hence, for the improvement of our elution strategy, we increased sodium chloride and sodium phosphate buffer concentration to 750 mM and applied detergents in desorption buffers while they bind strongly to matrix, promoting a selective elution of our biomolecule. The choice of detergent for purification trials was based in previous study about solubilization focusing the influence of detergent selection in STEAP1 yields. This study demonstrates that Triton X-100 was the best detergent, though is a mild and cheap chaotropic agent often used in membrane protein isolation.

3. STEAP1 isolation on Octyl-Sepharose

Octyl-Sepharose is a well-established and highly hydrophobic resin for capture and intermediate purification of larger proteins, resulting of a higher length in the alkyl chain. Is made of highly cross-linked agarose beads, which offer an excellent flow property to the medium (115) (152).

Initial trials described above showed that application of lower concentration of salts in mobile phase did not contribute to protein target elution being necessary also the application of a specific detergent. So, to optimize the chromatographic strategy, the adjustment of salt and detergent concentration is necessary to allow STEAP1 total retention and elution, respectively. STEAP1 isolation strategy comprises cells lysates load at high sodium phosphate buffer and sodium chloride (table 3) concentrations to promote protein retention, followed by a 50mM sodium phosphate buffer step to remove moderate hydrophobic and weakly retained protein contaminants. The next step was the increasing detergent gradient until 1% in order to screening the favorable Triton X-100 concentration to promote elution of the target protein. In the last step, we apply 1% of Triton to elute totally the high hydrophobic components that may still in the column. Chromatographic assays performed for STEAP1 purification optimization are summarized in table 3.

Table 3 - Summary of salt, Triton X-100 used in detergent gradient, and STEAP1 elution behavior onto an Octyl-Sepharose support.

	[Sodium Phosphate Buffer] Concentrations (mM)	[Sodium Chloride] Concentrations (mM)	STEAP1 Retention	STEAP1 Elution Behaviour	
				Sodium Phosphate Buffer (50 mM)	Triton X-100 (0-1%)
Chromatographic methodologies	1000		+++	-	+++
	750		+	+	+
	600		+	-	+
		750	-	-	

(−) to (+) denotes respectively no retention/retention and no elution/elution of STEAP1 on Octyl-Sepharose

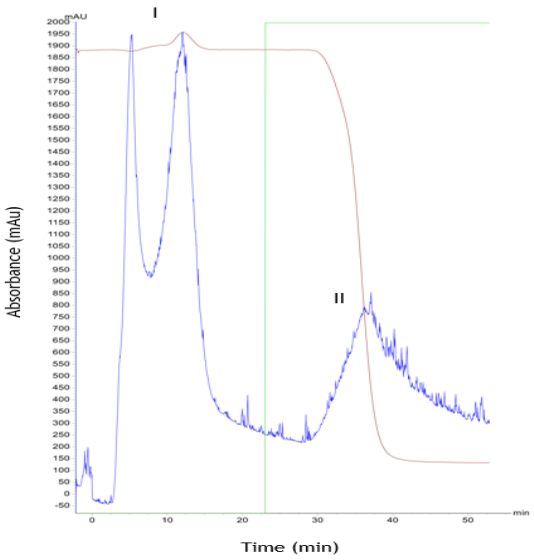

Figure 16. Chromatographic profile of STEAP1 isolation trials on Octyl-Sepharose. Adsorption was performed at 750 mM sodium chloride, pH 8.0 followed by 50 mM sodium phosphate buffer step. Blue line represents the absorbance at 280 nm, green line the sodium phosphate buffer concentration in mobile phase, and the brown line the conductivity.

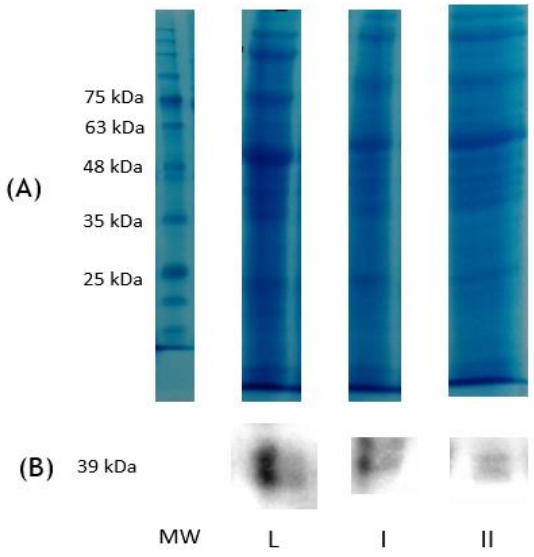

Figure 17. SDS-PAGE (A) and Western Blot (B) analysis of samples collected on STEAP1 isolation chromatographic assay [figure 16]. Lane MW – molecular weight standards; Lane L – solubilized lysis pellet; Lane I – Peaks I obtained at 750 mM sodium chloride; Lane II – Peak II obtained with 50Mm sodium phosphate buffer.

Contrary to what was expected, by SDS-PAGE and Western Blot analysis (figure 17) of samples collected from the chromatographic profile (figure 16) with the increase of sodium chloride concentration to 750 mM, STEAP1 retention onto the matrix decreased and was a weak pattern expression in elution at peak II, so this approach was discarded.

After the screening of an adequate STEAP1 adsorption strategy, was tried to optimize a suitable chromatographic strategy for its isolation. So, STEAP1 chromatographic isolation was achieved with salt and detergent concentrations mentioned under in figure 18. Adsorption was performed at 1000 mM sodium phosphate buffer, followed by 50 mM sodium phosphate buffer step. Desorption was performed at 1% Triton X-100. So, with application of moderate to high sodium phosphate buffer concentrations, contaminations are effectively removed by pass-through on column, while hydrophobic adsorption of loaded protein is consolidated (155-156). By SDS-PAGE and Western Blot analysis (figure 19), we confirm the hypothesis that for complete STEAP1 retention are required sodium phosphate concentrations above 500 mM and with 1000 mM we achieve a total adsorption of the protein to the resin. Consequently, the elution must be performed with increasing concentrations of Triton X-100 1% in 50 mM sodium phosphate buffer, where in peak IV there is a presence of STEAP1 immunodomain single band with correct molecular weight 39 kDa. This mechanism can be explained due the fact of protein position in the column influences the interaction in Octyl-Sepharose, since when a more hydrophobic zone is oriented to the stationary phase, like hydrophobic tail responsible for cellular membrane connection, is created a stronger interaction and thus is necessary an aggressive elution (136-137). Therefore, on the experiment conditions stated above, considerable amounts of purified STEAP1 were eluted.

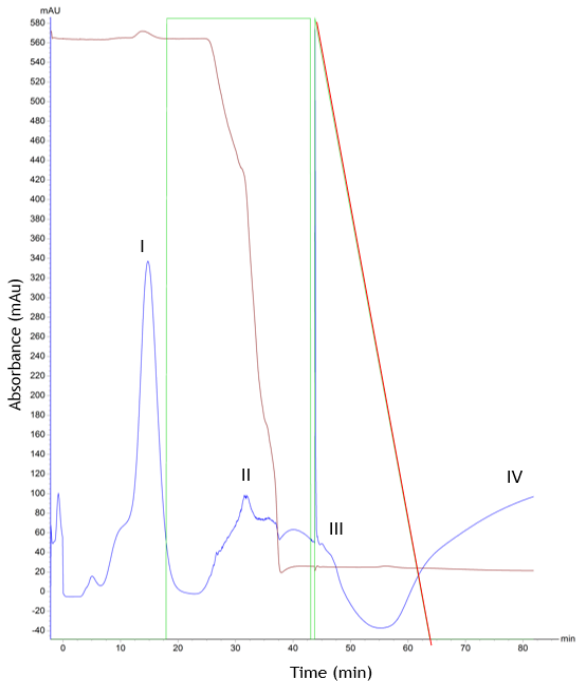

Figure 18. Chromatographic profile of STEAP1 isolation on Octyl-Sepharose. Adsorption was performed at 1000 mM sodium phosphate buffer, pH 8.0 followed by 50 mM sodium phosphate buffer step. Desorption was performed at 1% Triton X-100, pH 8.0. Blue line represents the absorbance at 280 nm, green line the sodium phosphate buffer concentration in mobile phase, red line the Triton X-100 percentage in mobile phase and the brown line the conductivity.

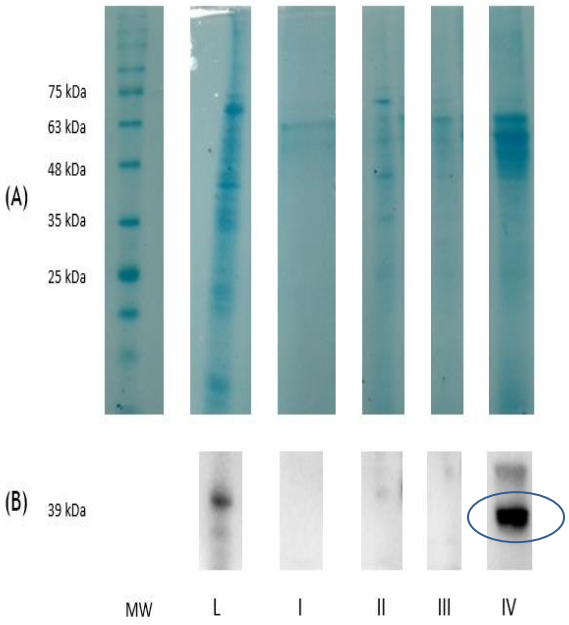

Figure 19. SDS-PAGE (A) and Western Blot (B) analysis of samples collected on STEAP1 isolation chromatographic assay [figure 18]. Lane MW – molecular weight standards; Lane L – solubilized lysis pellet; Lane I – Peaks I obtained at 1000 mM sodium chloride; Lane II – Peak II obtained with 50 mM sodium phosphate buffer. Lanes III and IV – Peaks III and IV obtained at linear gradient of 1% Triton X-100.

Since sodium phosphate precipitates at concentrations above 150 mM at 4°C, purification trials had to be carried out at room temperature. This may be a limitation if we are working with a thermolabile protein or susceptible to proteolysis (phenomenon that minimize at low temperatures) (154). On the other hand, low temperatures may weaken hydrophobic interactions which is prejudicial to cold-sensitive proteins (154) (157). So, we develop a complementary strategy to isolate STEAP1 without hitches both at the laboratory and/or protein structural level. A combination of two salting-out salts (termed "dual salt system") has a remarkable benefit on protein solubility and binding of a given protein to HIC resin (111) (155) (157). The salting-out effects are related to the molar concentration of the salts, and accordingly the literature, combining two different salts would be expected to be additive in prevent salt precipitation (158). We have examined the effects of dual salt system such monosodium phosphate buffer with sodium chloride on HIC binding and reported their synergistic behavior (Table 4).

Table 4 - Summary of salt dual system, Triton X-100 used in detergent gradient, and STEAP1 elution behavior onto an Octyl-Sepharose support.

	[Monosodium phosphate + Sodium chloride] Concentrations (mM)	STEAP1 Retention	STEAP1 Elution Behaviour		
			Sodium Phosphate Buffer (50 mM)	Triton X-100 Linear Gradient (0-1%)	Triton X-100 Step Gradient (0-0.5%-1%)
Chromatographic methodologies	750	+	-	+	
	750	+	-		+
	600	-	-	-	
	600	-	-		-
	500	-	-		

(−) to (+) denotes respectively no retention/retention and no elution/elution of STEAP1 on Octyl-Sepharose

Through analysis of Table 4, we observed similar results as approaches with one salt described above. There is a need of concentrations above 600 mM of monosodium phosphate buffer plus sodium chloride to complete retention of STEAP1 onto the matrix. Consequently, as with only one salt, if the adsorption is achieved at high concentrations, the elution must be performed with increasing concentrations of Triton X-100 in 50 mM phosphate buffer both in linear and step gradient.

The STEAP1 isolation was achieved with the application of a dual salt system approach, using monosodium phosphate plus sodium chloride at 750 mM in mobile phase followed with desorption in a linear and step gradient of 1% Triton X-100 respectively demonstrated in chromatographic profiles of figure 20 (A) and (B).

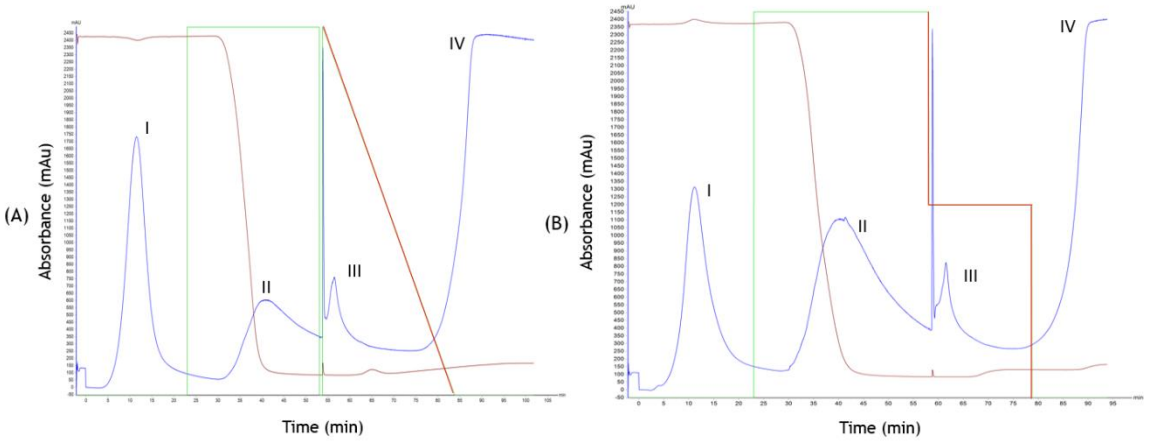

Figure 20. Chromatographic profiles of STEAP1 isolation trials on Octyl-Sepharose. Adsorption was performed at 750 mM monosodium phosphate plus sodium chloride, pH 8.0 followed by 50 mM sodium phosphate buffer step. Desorption was performed in linear gradient (A) and step gradient (B) of 1% Triton X-100, pH 8.0. Blue line represents the absorbance at 280 nm, green line the monosodium phosphate with sodium chloride concentration in mobile phase, red line the Triton X-100 percentage in mobile phase and the brown line the conductivity.

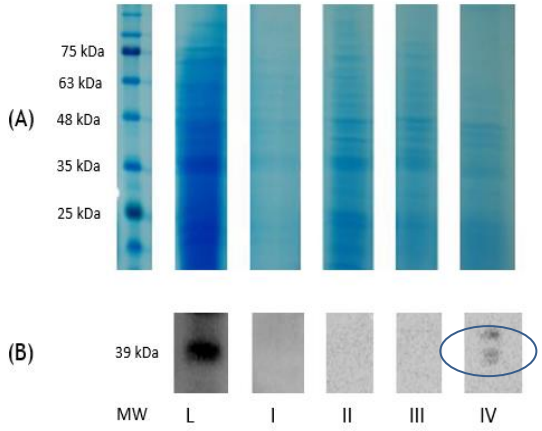

Figure 21. SDS-PAGE (A) and Western Blot (B) analysis of samples collected on STEAP1 isolation chromatographic assay [figure 20 (A)]. Lane MW – molecular weight standards; Lane L – solubilized lysis; Lane I – Peaks I obtained at 750 mM monosodium phosphate plus sodium chloride; Lane II – Peak II obtained with 50 mM sodium phosphate buffer; Lanes III and IV – Peaks III and IV obtained at linear gradient of 1% Triton X-100.

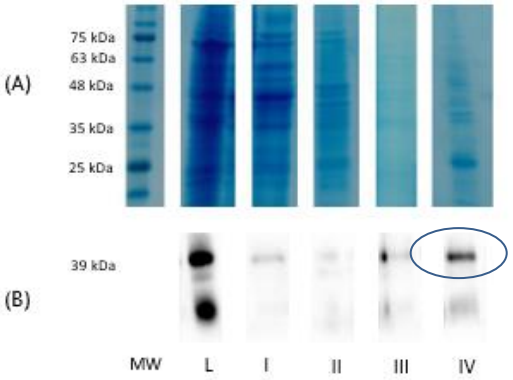

Figure 22. SDS-PAGE (A) and Western Blot (B) analysis of samples collected on STEAP1 isolation chromatographic assay [figure 20 (B)]. Lane MW – molecular weight standards; Lane L – solubilized lysis pellet; Lane I – Peaks I obtained at 750 mM monosodium phosphate plus sodium chloride; Lane II – Peak II obtained with 50 mM sodium phosphate buffer; Lanes III and IV – Peaks III and IV obtained at step gradient of 1% Triton X-100.

By SDS-PAGE and Western Blot analysis (figure 21 and 22), we confirm the achievement of STEAP1 isolation with dual salt system where in peak IV considerable amounts of purified STEAP1 were eluted with correct molecular weight 39 kDa.

4. STEAP1 purification on Butyl-Sepharose

Butyl-Sepharose is an intermediate hydrophobic resin, with lower length in the alkyl chain in comparison with Octyl-Sepharose, and for this reason show highest levels of selectivity (159). According to these characteristics, it is expectable that dual-salt concentration to be used in mobile phase will be the same or slightly higher than that used in Octyl-experiments. Also, it was verified that in spite of mild retention conditions, it is necessary high detergent concentrations to promote STEAP1 elution. First experiments are summarized in table 5 considering required salt and detergent concentrations and protein behaviour.

Table 5 - Summary of salt dual system, Triton X-100 used in detergent gradient, and STEAP1 elution behavior onto an Butyl-Sepharose support.

	[Monosodium phosphate + Sodium chloride] Concentrations (mM)	STEAP1 Retention	STEAP1 Elution Behaviour		
			Sodium Phosphate Buffer (50 mM)	Triton X-100 Linear Gradient (0-1%)	Triton X-100 Step Gradient (0-0.5%-1%)
Chromatographic methodologies	800	+	-	+	
	750	+	-	Residual	
	750	+	-		+
	600	-	-	-	

(−) to (+) denotes respectively no retention/retention and no elution/elution of STEAP1 on Butyl-Sepharose

The chromatographic profiles of STEAP1 with application of the same dual salt conditions referred above, using 750 mM of monosodium phosphate plus sodium chloride in mobile phase followed with desorption in linear and step gradient of 1% Triton X-100, are respectively demonstrated at figure 23 (A) and (B).

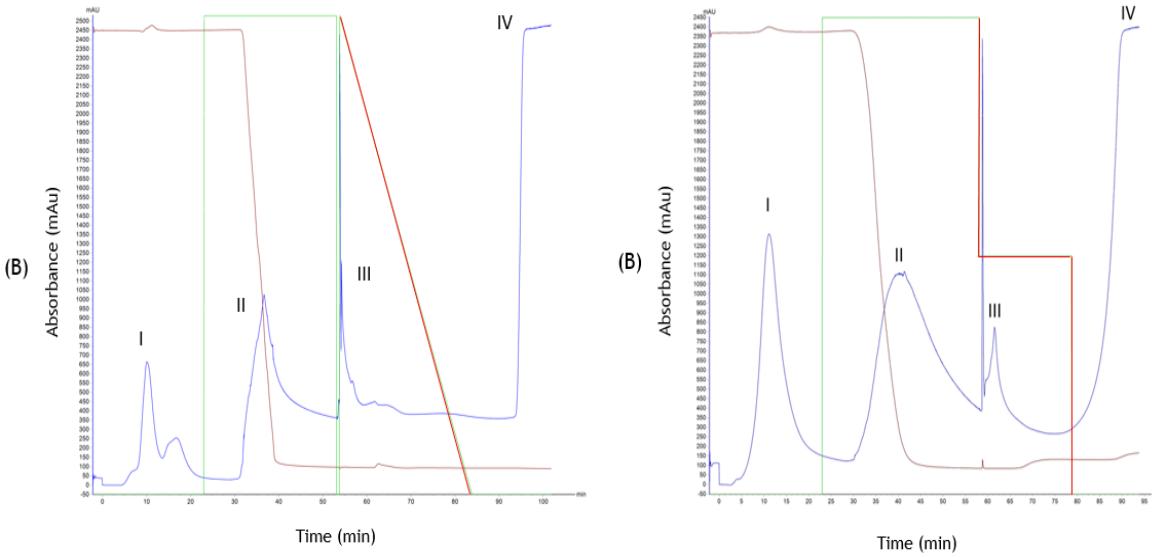

Figure 23. Chromatographic profiles of STEAP1 isolation trials on Butyl-Sepharose. Adsorption was performed at 750 mM monosodium phosphate with sodium chloride, pH 8.0 followed by 50 mM sodium phosphate buffer step. Desorption was performed in linear gradient (A) and step gradient (B) of 1% Triton X-100, pH 8.0. Blue line represents the absorbance at 280 nm, green line the monosodium phosphate with sodium chloride concentration in mobile phase, red line the Triton X-100 percentage in mobile phase and the brown line the conductivity.

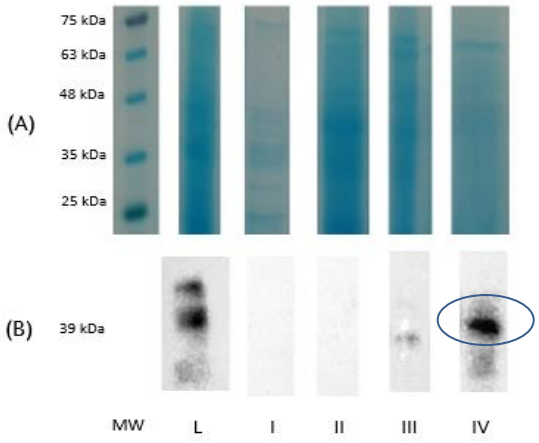

Figure 24. SDS-PAGE (A) and Western Blot (B) analysis of samples collected on STEAP1 isolation chromatographic assay [figure 23 (A)]. Lane MW – molecular weight standards; Lane L – solubilized lysis pellet; Lane I – Peaks I obtained at 750 mM monosodium phosphate with sodium chloride; Lane II – Peak II obtained with 50 mM sodium phosphate buffer; Lanes III and IV – Peaks III and IV obtained at linear gradient of 1% Triton X-100.

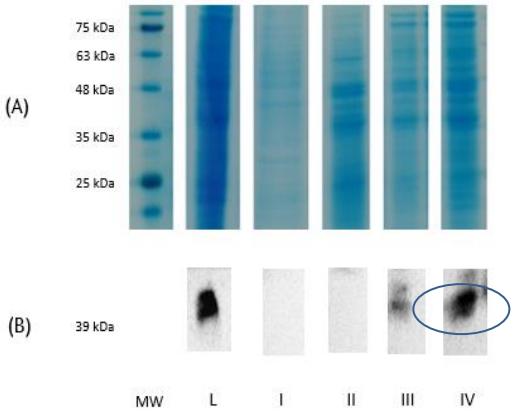

Figure 25. SDS-PAGE (A) and Western Blot (B) analysis of samples collected on STEAP1 isolation chromatographic assay [figure 23 (B)]. Lane MW – molecular weight standards; Lane L – solubilized lysis pellet; Lane I – Peaks I obtained at 750 mM monosodium phosphate with sodium chloride; Lane II – Peak II obtained with 50 mM sodium phosphate buffer; Lanes III and IV – Peaks III and IV obtained at step gradient of 1% Triton X-100.

As seen in figure 23 and 26, the chromatographic profiles showed four peaks of interest. Western Blot analysis [figure 24, 25 and 27 (B)], was carried out to confirm the immunological activity of the protein and it was confirmed the presence of STEAP1 immunodomain single bands with correct molecular weight (39kDa) in the peaks where was applied Triton X-100 to perform elution.

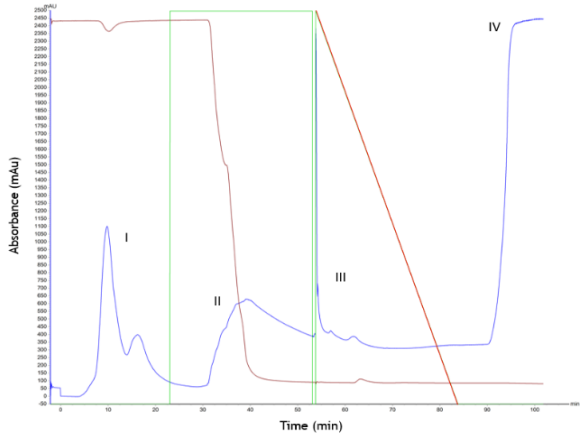

Figure 26. Chromatographic profile of STEAP1 isolation trial on Butyl-Sepharose. Adsorption was performed at 800 mM monosodium phosphate with sodium chloride, pH 8.0 followed by 50 mM sodium phosphate buffer step. Desorption was performed in linear gradient of 1% Triton X-100, pH 8.0. Blue line represents the absorbance at 280 nm, green line the monosodium phosphate with sodium chloride concentration in mobile phase, red line the Triton X-100 percentage in mobile phase and the brown line the conductivity.

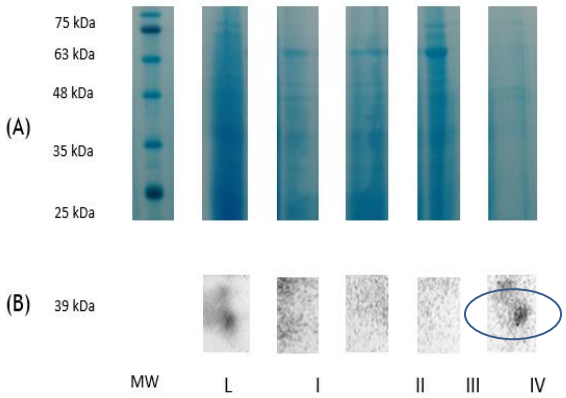

Figure 27. SDS-PAGE (A) and Western Blot (B) analysis of samples collected on STEAP1 isolation chromatographic assay [figure 26]. Lane MW – molecular weight standards; Lane L – solubilized lysis pellet; Lane I – Peaks I obtained at 800 mM monosodium phosphate with sodium chloride; Lane II – Peak II obtained with 50Mm sodium phosphate buffer; Lanes III and IV – Peaks III and IV obtained at linear gradient of 1% Triton X-100.

Chapter 5

Conclusion and Future Perspectives

At present, the knowledge of transmembrane proteins isolation is crucial due to its role in the development of novel therapeutic tools for several human pathologies. Over several years, chromatographic separation procedures were used in membrane proteins purification. Nevertheless, there are no studies in literature focused in STEAP1 isolation and, therefore, a comprehensive and exhaustive study had to be done.

For the first time, it was possible the STEAP1 isolation in two hydrophobic adsorbents Octyl- and Butyl-Sepharose by Hydrophobic Interaction Chromatography. In overall, the isolation of the protein is possible with suitable adjusts on parameters such type of salt and respective ionic strength.

Concerning the recovery step, this was complete easily by solubilization with 1 % (v/v) of a non-ionic detergent, Triton X-100, since it demonstrated to be the most suitable between other five tested and promoted high levels of recovery. Some membrane proteins are soluble only in a single detergent species that fulfills specific solubilization requirements, while others are soluble in many different detergents but are only functionally active in one of them. Another structures that are able to produce a hydrophobic surrounding environment being similar to the native lipid bilayer, such as liposomes, reverse-micelles or nanolipoproteins could also be tested.

First chromatographic screening trials on Octyl-Sepharose demonstrated that salt and detergent applications on mobile phase are crucial to, respectively, STEAP1 adsorption and elution. Intermediate to high sodium phosphate concentrations are also required to protein adsorption. Also, it was verified that after this chromatographic step in both matrices at high salt concentrations there are a tendency for salt precipitate during the concentration process. So, is highly desirable the use of another type of salt to protein isolation, such application of dual salt system. On the other hand, are expected that Octyl-Sepharose, despite of its high hydrophobicity, allows high protein recovery and excellent selectivity using only mild salt conditions. Furthermore, application of a specific detergent is necessary to STEAP1 elution, being detergent concentration also similar to each resin. Optimization of chromatographic procedure is an empirical method, that is slow and time-consuming and depends on several parameters such as temperature, pH, ionic strength, salt type and detergent characteristics that affect hydrophobic interactions on HIC, which may influence protein stability and structure.

In the future the use of Epoxy-Sepharose could be also evaluated, since this matrix is a mild hydrophobic adsorbent, with lower selective retention, which use of these mild hydrophobic ligands appears to be a promising substitute to strongly bound protein elution since permit an adequate binding strength and weaker elution conditions, without use of chaotropic agents, leading to faster chromatographic cycles.

Although successful applications of HIC in the purification of integral membrane proteins are uncommon, our results indicate that traditional hydrophobic matrices are a promising alternative for the isolation of STEAP1.

References

1. Aaron L, Franco OE, Hayward SW. Review of prostate anatomy and embryology and the etiology of benign prostatic hyperplasia. Urologic Clinics. 2016;43(3):279-88.
2. Lee CH, Akin-Olugbade O, Kirschenbaum A. Overview of prostate anatomy, histology, and pathology. Endocrinology and Metabolism Clinics. 2011;40(3):565-75.
3. Selman SH. The McNeal prostate: a review. Urology. 2011;78(6):1224-8.
4. Hammerich KH, Ayala GE, Wheeler TM. Anatomy of the prostate gland and surgical pathology of prostate cancer. Cambridge University, Cambridge. 2009:1-10.
5. Fine SW, Reuter VE. Anatomy of the prostate revisited: implications for prostate biopsy and zonal origins of prostate cancer. Histopathology. 2012;60(1):142-52.
6. Ayala AG, Ro JY, Babaian R, Troncoso P, Grignon DJ. The prostatic capsule: does it exist? Its importance in the staging and treatment of prostatic carcinoma. The American journal of surgical pathology. 1989;13(1):21-7.
7. Timms BG. Prostate development: a historical perspective. Differentiation. 2008;76(6):565-77.
8. Bhavsar A, Verma S. Anatomic imaging of the prostate. BioMed research international. 2014;2014.
9. Chodak GW, Kranc DM, Puy LA, Takeda H, Johnson K, Chang C. Nuclear localization of androgen receptor in heterogeneous samples of normal, hyperplastic and neoplastic human prostate. The Journal of urology. 1992;147(3):798-803.
10. Shen MM, Abate-Shen C. Molecular genetics of prostate cancer: new prospects for old challenges. Genes & development. 2010;24(18):1967-2000.
11. Kumar V, Majumder P. Prostate gland: structure, functions and regulation. International urology and nephrology. 1995;27(3):231-43.
12. Siegel RL, Miller KD, Jemal A. Cancer statistics, 2018. CA: a cancer journal for clinicians. 2018;68(1):7-30.
13. Marugame T, Katanoda K. International comparisons of cumulative risk of breast and prostate cancer, from cancer incidence in five continents Vol. VIII. Japanese journal of clinical oncology. 2006;36(6):399-400.
14. Torre LA, Bray F, Siegel RL, Ferlay J, Lortet-Tieulent J, Jemal A. Global cancer statistics, 2012. CA: a cancer journal for clinicians. 2015;65(2):87-108.
15. Pina F, Castro C, Ferro A, Bento MJ, Lunet N. Prostate cancer incidence and mortality in Portugal: trends, projections and regional differences. European Journal of Cancer Prevention. 2017;26(5):404-10.
16. Giovannucci E, Liu Y, Platz EA, Stampfer MJ, Willett WC. Risk factors for prostate cancer incidence and progression in the health professionals follow-up study.

International journal of cancer. 2007;121(7):1571-8.
17. Patel AR, Klein EA. Risk factors for prostate cancer. Nature Reviews Urology. 2009;6(2):87.
18. Bostwick DG, Burke HB, Djakiew D, Euling S, Ho Sm, Landolph J, et al. Human prostate cancer risk factors. Cancer. 2004;101(S10):2371-490.
19. Grönberg H. Prostate cancer epidemiology. The Lancet. 2003;361(9360):859-64.
20. Bratt O. Hereditary prostate cancer. BJU international. 2000;85(5):588-98.
21. Hoffman RM, Gilliland FD, Eley JW, Harlan LC, Stephenson RA, Stanford JL, et al. Racial and ethnic differences in advanced-stage prostate cancer: the Prostate Cancer Outcomes Study. Journal of the National Cancer Institute. 2001;93(5):388-95.
22. Kumar B, Koul S, Khandrika L, Meacham RB, Koul HK. Oxidative stress is inherent in prostate cancer cells and is required for aggressive phenotype. Cancer research. 2008;68(6):1777-85.
23. Khandrika L, Kumar B, Koul S, Maroni P, Koul HK. Oxidative stress in prostate cancer. Cancer letters. 2009;282(2):125-36.
24. Gann PH, Hennekens CH, Ma J, Longcope C, Stampfer MJ. Prospective study of sex hormone levels and risk of prostate cancer. JNCI: Journal of the National Cancer Institute. 1996;88(16):1118-26.
25. Ingles SA, Ross RK, Yu MC, Haile RW, Irvine RA, La Pera G, et al. Association of prostate cancer risk with genetic polymorphisms in vitamin D receptor and androgen receptor. Journal of the National Cancer Institute. 1997;89(2):166-70.
26. Giovannucci E, Rimm EB, Colditz GA, Stampfer MJ, Ascherio A, Chute CC, et al. A prospective study of dietary fat and risk of prostate cancer. JNCI: Journal of the National Cancer Institute. 1993;85(19):1571-9.
27. Hayes RB, Ziegler RG, Gridley G, Swanson C, Greenberg RS, Swanson GM, et al. Dietary factors and risks for prostate cancer among blacks and whites in the United States. Cancer Epidemiology and Prevention Biomarkers. 1999;8(1):25-34.
28. De Pergola G, Silvestris F. Obesity as a major risk factor for cancer. Journal of obesity. 2013;2013.
29. Prins GS. Endocrine disruptors and prostate cancer risk. Endocrine-related cancer. 2008;15(3):649-56.
30. Soto AM, Sonnenschein C. Environmental causes of cancer: endocrine disruptors as carcinogens. Nature Reviews Endocrinology. 2010;6(7):363.
31. Diamanti-Kandarakis E, Bourguignon J-P, Giudice LC, Hauser R, Prins GS, Soto AM, et al. Endocrine-disrupting chemicals: an Endocrine Society scientific statement. Endocrine reviews. 2009;30(4):293-342.

32. Shand RL, Gelmann EP. Molecular biology of prostate-cancer pathogenesis. Current opinion in urology. 2006;16(3):123-31.
33. Gonzalgo ML, Isaacs WB. Molecular pathways to prostate cancer. The Journal of urology. 2003;170(6):2444-52.
34. Bostwick DG. The pathology of early prostate cancer. CA: a cancer journal for clinicians. 1989;39(6):376-93.
35. De Marzo AM, Platz EA, Sutcliffe S, Xu J, Grönberg H, Drake CG, et al. Inflammation in prostate carcinogenesis. Nature Reviews Cancer. 2007;7(4):256.
36. Bostwick DG. Prostatic intraepithelial neoplasia. Current urology reports. 2000;1(1):65-70.
37. Qian J, Wollan P, Bostwick DG. The extent and multicentricity of high-grade prostatic intraepithelial neoplasia in clinically localized prostatic adenocarcinoma. Human pathology. 1997;28(2):143-8.
38. Bostwick DG, Brawer MK. Prostatic intra-epithelial neoplasia and early invasion in prostate cancer. Cancer. 1987;59(4):788-94.
39. Yang RM, Naitoh J, Murphy M, Wang H-j, Phillipson J, Dekernion JB, et al. Low p27 expression predicts poor disease-free survival in patients with prostate cancer. The Journal of urology. 1998;159(3):941-5.
40. Li J, Yen C, Liaw D, Podsypanina K, Bose S, Wang SI, et al. PTEN, a putative protein tyrosine phosphatase gene mutated in human brain, breast, and prostate cancer. science. 1997;275(5308):1943-7.
41. Ouyang X, DeWeese TL, Nelson WG, Abate-Shen C. Loss-of-function of Nkx3. 1 promotes increased oxidative damage in prostate carcinogenesis. Cancer research. 2005;65(15):6773-9.
42. Waris G, Ahsan H. Reactive oxygen species: role in the development of cancer and various chronic conditions. Journal of carcinogenesis. 2006;5:14.
43. Dranoff G. Cytokines in cancer pathogenesis and cancer therapy. Nature Reviews Cancer. 2004;4(1):11.
44. Condeelis J, Pollard JW. Macrophages: obligate partners for tumor cell migration, invasion, and metastasis. Cell. 2006;124(2):263-6.
45. Denmeade SR, Lin XS, Isaacs JT. Role of programmed (apoptotic) cell death during the progression and therapy for prostate cancer. The Prostate. 1996;28(4):251-65.
46. Crawford ED, Petrylak D. Castration-resistant prostate cancer: descriptive yet pejorative? Journal of Clinical Oncology. 2010;28(23):e408-e.
47. Saraon P, Jarvi K, Diamandis EP. Molecular alterations during progression of prostate cancer to androgen independence. Clinical chemistry. 2011;57(10):1366-75.
48. Scardino PT, Weaver R, M'Liss AH. Early detection of prostate cancer. Human

pathology. 1992;23(3):211-22.
49. Heidenreich A, Bellmunt J, Bolla M, Joniau S, Mason M, Matveev V, et al. EAU guidelines on prostate cancer. Part 1: screening, diagnosis, and treatment of clinically localised disease. European urology. 2011;59(1):61-71.
50. Lassen P, Thompson I. Treatment options for prostate cancer. Urologic nursing. 1994;14(1):12-5.
51. Bill-Axelson A, Holmberg L, Ruutu M, Häggman M, Andersson S-O, Bratell S, et al. Radical prostatectomy versus watchful waiting in early prostate cancer. New England journal of medicine. 2005;352(19):1977-84.
52. Stamey TA, Yang N, Hay AR, McNeal JE, Freiha FS, Redwine E. Prostate-specific antigen as a serum marker for adenocarcinoma of the prostate. New England Journal of Medicine. 1987;317(15):909-16.
53. Chu M. Prostate-specific antigen and early detection of prostate cancer. Tumor biology. 1997;18(2):123-34.
54. Presti JC, Hovey R, Bhargava V, Carroll PR, Shinohara K. Prospective evaluation of prostate specific antigen and prostate specific antigen density in the detection of carcinoma of the prostate: ethnic variations. The Journal of urology. 1997;157(3):907-12.
55. Partin AW, Yoo J, Carter HB, Pearson JD, Chan DW, Epstein JI, et al. The use of prostate specific antigen, clinical stage and Gleason score to predict pathological stage in men with localized prostate cancer. The Journal of urology. 1993;150(1):110-4.
56. Partin AW, Carter HB, Chan DW, Epstein JI, Oesterling JE, Rock RC, et al. Prostate specific antigen in the staging of localized prostate cancer: influence of tumor differentiation, tumor volume and benign hyperplasia. The Journal of urology. 1990;143(4):747-52.
57. Moul JW, Sesterhenn IA, Connelly RR, Douglas T, Srivastava S, Mostofi FK, et al. Prostate-specific antigen values at the time of prostate cancer diagnosis in African-American men. Jama. 1995;274(16):1277-81.
58. Arlen PM, Mohebtash M, Madan RA, Gulley JL. Promising novel immunotherapies and combinations for prostate cancer. 2009.
59. May KF, Gulley JL, Drake CG, Dranoff G, Kantoff PW. Prostate cancer immunotherapy. Clinical Cancer Research. 2011;17(16):5233-8.
60. Ercole CJ, Lange PH, Mathisen M, Chiou RK, Reddy PK, Vessella RL. Prostatic specific antigen and prostatic acid phosphatase in the monitoring and staging of patients with prostatic cancer. The Journal of urology. 1987;138(5):1181-4.
61. Foti AG, Cooper JF, Herschman H, Malvaez RR. Detection of prostatic cancer by

solid-phase radioimmunoassay of serum prostatic acid phosphatase. New England Journal of Medicine. 1977;297(25):1357-61.
62. Ghosh A, Heston WD. Tumor target prostate specific membrane antigen (PSMA) and its regulation in prostate cancer. Journal of cellular biochemistry. 2004;91(3):528-39.
63. Xiao Z, Adam B-L, Cazares LH, Clements MA, Davis JW, Schellhammer PF, et al. Quantitation of serum prostate-specific membrane antigen by a novel protein biochip immunoassay discriminates benign from malignant prostate disease. Cancer research. 2001;61(16):6029-33.
64. Beckett ML, Cazares LH, Vlahou A, Schellhammer PF, Wright GL. Prostate-specific membrane antigen levels in sera from healthy men and patients with benign prostate hyperplasia or prostate cancer. Clinical cancer research. 1999;5(12):4034-40.
65. Reiter RE, Gu Z, Watabe T, Thomas G, Szigeti K, Davis E, et al. Prostate stem cell antigen: a cell surface marker overexpressed in prostate cancer. Proceedings of the National Academy of Sciences. 1998;95(4):1735-40.
66. Gu Z, Thomas G, Yamashiro J, Shintaku I, Dorey F, Raitano A, et al. Prostate stem cell antigen (PSCA) expression increases with high gleason score, advanced stage and bone metastasis in prostate cancer. Oncogene. 2000;19(10):1288.
67. Zha S, Ferdinandusse S, Denis S, Wanders RJ, Ewing CM, Luo J, et al. α-Methylacyl-CoA racemase as an androgen-independent growth modifier in prostate cancer. Cancer Research. 2003;63(21):7365-76.
68. Jiang Z, Wu C, Woda B, Iczkowski K, Chu P, Tretiakova M, et al. Alpha-methylacyl-CoA racemase: a multi-institutional study of a new prostate cancer marker. Histopathology. 2004;45(3):218-25.
69. Rubin MA, Zhou M, Dhanasekaran SM, Varambally S, Barrette TR, Sanda MG, et al. α-Methylacyl coenzyme A racemase as a tissue biomarker for prostate cancer. Jama. 2002;287(13):1662-70.
70. Paul B, Dhir R, Landsittel D, Hitchens MR, Getzenberg RH. Detection of prostate cancer with a blood-based assay for early prostate cancer antigen. Cancer research. 2005;65(10):4097-100.
71. Leman ES, Cannon GW, Trock BJ, Sokoll LJ, Chan DW, Mangold L, et al. RETRACTED: EPCA-2: A Highly Specific Serum Marker for Prostate Cancer. Elsevier; 2007.
72. Jerónimo C, Usadel H, Henrique R, Oliveira J, Lopes C, Nelson WG, et al. Quantitation of GSTP1 methylation in non-neoplastic prostatic tissue and organ-confined prostate adenocarcinoma. Journal of the National Cancer Institute. 2001;93(22):1747-52.
73. Brooks JD, Weinstein M, Lin X, Sun Y, Pin SS, Bova GS, et al. CG island methylation changes near the GSTP1 gene in prostatic intraepithelial neoplasia. Cancer Epidemiology

and Prevention Biomarkers. 1998;7(6):531-6.
74. Cairns P, Esteller M, Herman JG, Schoenberg M, Jeronimo C, Sanchez-Cespedes M, et al. Molecular detection of prostate cancer in urine by GSTP1 hypermethylation. Clinical Cancer Research. 2001;7(9):2727-30.
75. Simon J-P, Aunis D. Biochemistry of the chromogranin A protein family. Biochemical Journal. 1989;262(1):1.
76. Helman LJ, Ahn T, Levine M, Allison A, Cohen PS, Cooper MJ, et al. Molecular cloning and primary structure of human chromogranin A (secretory protein I) cDNA. Journal of Biological Chemistry. 1988;263(23):11559-63.
77. Isshiki S, Akakura K, Komiya A, Suzuki H, Kamiya N, Ito H. Chromogranin a concentration as a serum marker to predict prognosis after endocrine therapy for prostate cancer. The Journal of urology. 2002;167(2):512-5.
78. Ferrero-Poüs M, Hersant A, Pecking A, Brésard-Leroy M, Pichon M. Serum chromogranin-A in advanced prostate cancer. BJU international. 2001;88(7):790-6.
79. Fracalanza S, Prayer-Galetti T, Pinto F, Navaglia F, Sacco E, Ciaccia M, et al. Plasma chromogranin A in patients with prostate cancer improves the diagnostic efficacy of free/total prostate-specific antigen determination. Urologia internationalis. 2005;75(1):57-61.
80. Gomes IM, Maia CJ, Santos CR. STEAP proteins: from structure to applications in cancer therapy. Molecular Cancer Research. 2012;10(5):573-87.
81. Finegold AA, Shatwell KP, Segal AW, Klausner RD, Dancis A. Intramembrane bis-heme motif for transmembrane electron transport conserved in a yeast iron reductase and the human NADPH oxidase. Journal of Biological Chemistry. 1996;271(49):31021-4.
82. Barroca-Ferreira J, Pais J, Santos M, Gonçalves A, Gomes I, Sousa I, et al. Targeting STEAP1 protein in human cancer: current trends and future challenges. Current cancer drug targets. 2018;18(3):222-30.
83. Ohgami RS, Campagna DR, McDonald A, Fleming MD. The Steap proteins are metalloreductases. Blood. 2006;108(4):1388-94.
84. Grunewald TG, Bach H, Cossarizza A, Matsumoto I. The STEAP protein family: versatile oxidoreductases and targets for cancer immunotherapy with overlapping and distinct cellular functions. Biology of the Cell. 2012;104(11):641-57.
85. Gomes IM, Santos CR, Maia CJ. Expression of STEAP1 and STEAP1B in prostate cell lines, and the putative regulation of STEAP1 by post-transcriptional and post-translational mechanisms. Genes & cancer. 2014;5(3-4):142.
86. Hubert RS, Vivanco I, Chen E, Rastegar S, Leong K, Mitchell SC, et al. STEAP: a prostate-specific cell-surface antigen highly expressed in human prostate tumors.

Proceedings of the National Academy of Sciences. 1999;96(25):14523-8.
87. Challita-Eid PM, Morrison K, Etessami S, An Z, Morrison KJ, Perez-Villar JJ, et al. Monoclonal antibodies to six-transmembrane epithelial antigen of the prostate-1 inhibit intercellular communication in vitro and growth of human tumor xenografts in vivo. Cancer Research. 2007;67(12):5798-805.
88. Grunewald TG, Diebold I, Esposito I, Plehm S, Hauer K, Thiel U, et al. STEAP1 is associated with the invasive and oxidative stress phenotype of Ewing tumors. Molecular cancer research. 2012;10(1):52-65.
89. Moreaux J, Kassambara A, Hose D, Klein B. STEAP1 is overexpressed in cancers: a promising therapeutic target. Biochemical and biophysical research communications. 2012;429(3):148-55.
90. Papaioannou NE, Beniata OV, Vitsos P, Tsitsilonis O, Samara P. Harnessing the immune system to improve cancer therapy. Annals of translational medicine. 2016;4(14).
91. Agarwal N, Padmanabh S, Vogelzang NJ. Development of novel immune interventions for prostate cancer. Clinical genitourinary cancer. 2012;10(2):84-92.
92. Rodeberg DA, Nuss RA, Elsawa SF, Celis E. Recognition of six-transmembrane epithelial antigen of the prostate–expressing tumor cells by peptide antigen–induced cytotoxic T lymphocytes. Clinical cancer research. 2005;11(12):4545-52.
93. Alves PM, Faure O, Graff-Dubois S, Cornet S, Bolonakis I, Gross D-A, et al. STEAP, a prostate tumor antigen, is a target of human CD8+ T cells. Cancer Immunology, Immunotherapy. 2006;55(12):1515-23.
94. Krupa M, Canamero M, Gomez CE, Najera JL, Gil J, Esteban M. Immunization with recombinant DNA and modified vaccinia virus Ankara (MVA) vectors delivering PSCA and STEAP1 antigens inhibits prostate cancer progression. Vaccine. 2011;29(7):1504-13.
95. de la Luz Garcia-Hernandez M, Gray A, Hubby B, Kast WM. In vivo effects of vaccination with six-transmembrane epithelial antigen of the prostate: a candidate antigen for treating prostate cancer. Cancer Research. 2007;67(3):1344-51.
96. Lee AG. How lipids affect the activities of integral membrane proteins. Biochimica et Biophysica Acta (BBA)-Biomembranes. 2004;1666(1):62-87.
97. Carpenter EP, Beis K, Cameron AD, Iwata S. Overcoming the challenges of membrane protein crystallography. Current opinion in structural biology. 2008;18(5):581-6.
98. Niegowski D, Hedrén M, Nordlund P, Eshaghi S. A simple strategy towards membrane protein purification and crystallization. International journal of biological macromolecules. 2006;39(1-3):83-7.
99. White SH. The progress of membrane protein structure determination. Protein Science. 2004;13(7):1948-9.

100. Eshaghi S, Hedrén M, Nasser MIA, Hammarberg T, Thornell A, Nordlund P. An efficient strategy for high-throughput expression screening of recombinant integral membrane proteins. Protein Science. 2005;14(3):676-83.
101. Muller G. Towards 3D Structures of G Protein-Coupled Receptors A Multidisciplinary Approach. Current medicinal chemistry. 2000;7(9):861-88.
102. Gohon Y, Popot J-L. Membrane protein–surfactant complexes. Current opinion in colloid & interface science. 2003;8(1):15-22.
103. Rigaud J-L, Lévy D. Reconstitution of membrane proteins into liposomes. Methods in enzymology. 372: Elsevier; 2003. p. 65-86.
104. le Maire M, Champeil P, MÖller JV. Interaction of membrane proteins and lipids with solubilizing detergents. Biochimica et Biophysica Acta (BBA)-Biomembranes. 2000;1508(1):86-111.
105. Garavito RM, Ferguson-Miller S. Detergents as tools in membrane biochemistry. Journal of Biological Chemistry. 2001;276(35):32403-6.
106. Seddon AM, Curnow P, Booth PJ. Membrane proteins, lipids and detergents: not just a soap opera. Biochimica et Biophysica Acta (BBA)-Biomembranes. 2004;1666(1):105-17.
107. Dong M, Baggetto LG, Falson P, LeMaire M, Penin F. Complete removal and exchange of sodium dodecyl sulfate bound to soluble and membrane proteins and restoration of their activities, using ceramic hydroxyapatite chromatography. Analytical biochemistry. 1997;247(2):333-41.
108. Reis S, Moutinho CG, Matos C, de Castro B, Gameiro P, Lima JL. Noninvasive methods to determine the critical micelle concentration of some bile acid salts. Analytical biochemistry. 2004;334(1):117-26.
109. Luche S, Santoni V, Rabilloud T. Evaluation of nonionic and zwitterionic detergents as membrane protein solubilizers in two-dimensional electrophoresis. Proteomics. 2003;3(3):249-53.
110. Hjelmeland LM. A nondenaturing zwitterionic detergent for membrane biochemistry: design and synthesis. Proceedings of the National Academy of Sciences. 1980;77(11):6368-70.
111. Nunes V, Bonifácio M, Queiroz J, Passarinha L. Assessment of COMT isolation by HIC using a dual salt system and low temperature. Biomedical Chromatography. 2010;24(8):858-62.
112. Correia F, Santos F, Pedro A, Bonifácio M, Queiroz J, Passarinha L. Recovery of biological active catechol-O-methyltransferase isoforms from Q-sepharose. Journal of separation science. 2014;37(1-2):20-9.

113. Pedro AQ, Correia FF, Santos FM, Espírito-Santo G, Gonçalves AM, Bonifácio MJ, et al. Biosynthesis and purification of histidine-tagged human soluble catechol-O-methyltransferase. Journal of Chemical Technology and Biotechnology. 2016;91(12):3035-44.
114. Bannwarth M, Schulz GE. The expression of outer membrane proteins for crystallization. Biochimica et Biophysica Acta (BBA)-Biomembranes. 2003;1610(1):37-45.
115. Queiroz J, Tomaz C, Cabral J. Hydrophobic interaction chromatography of proteins. Journal of biotechnology. 2001;87(2):143-59.
116. Jungbauer A. Chromatographic media for bioseparation. Journal of Chromatography A. 2005;1065(1):3-12.
117. Chen J, Tetrault J, Ley A. Comparison of standard and new generation hydrophobic interaction chromatography resins in the monoclonal antibody purification process. Journal of Chromatography A. 2008;1177(2):272-81.
118. Bornhorst JA, Falke JJ. [16] Purification of proteins using polyhistidine affinity tags. Methods in enzymology. 326: Elsevier; 2000. p. 245-54.
119. Chaga GS. Twenty-five years of immobilized metal ion affinity chromatography: past, present and future. Journal of biochemical and biophysical methods. 2001;49(1-3):313-34.
120. Zatloukalová E, Kučerová Z. Separation of cobalt binding proteins by immobilized metal affinity chromatography. Journal of Chromatography B. 2004;808(1):99-103.
121. Mooney JT, Fredericks DP, Zhang C, Christensen T, Jespergaard C, Schiødt CB, et al. Purification of a recombinant human growth hormone by an integrated IMAC procedure. Protein expression and purification. 2014;94:85-94.
122. Jungbauer A, Hahn R. Ion-exchange chromatography. Methods in enzymology. 463: Elsevier; 2009. p. 349-71.
123. Yamamoto S, Nakanishi K, Matsuno R. Ion-exchange chromatography of proteins: CRC Press; 1988.
124. Janson J-C. Protein purification: principles, high resolution methods, and applications: John Wiley & Sons; 2012.
125. Fexby S, Bülow L. Hydrophobic peptide tags as tools in bioseparation. Trends in biotechnology. 2004;22(10):511-6.
126. Soni B, Trivedi U, Madamwar D. A novel method of single step hydrophobic interaction chromatography for the purification of phycocyanin from Phormidium fragile and its characterization for antioxidant property. Bioresource technology. 2008;99(1):188-94.
127. Warren BS, Kusk P, Wolford RG, Hager GL. Purification and stabilization of transcriptionally active glucocorticoid receptor. Journal of Biological Chemistry.

1996;271(19):11434-40.
128. Hrkal Z, Rejnkova J. Hydrophobic interaction chromatography of serum proteins on Phenyl-Sepharose CL-4B. Journal of Chromatography A. 1982;242(2):385-8.
129. Comings DE, Miguel G, Lesser BH. Nuclear proteins. VI. Fractionation of chromosomal non-histone proteins using hydrophobic chromatography. Biochimica et Biophysica Acta (BBA)-Nucleic Acids and Protein Synthesis. 1979;563(1):253-60.
130. Tomaz CT, Duarte D, Queiroz JA. Comparative study on the fractionation of cellulases on some hydrophobic interaction chromatography adsorbents. Journal of Chromatography A. 2002;944(1-2):211-6.
131. Hassl A, Aspöck H. Purification of egg yolk immunoglobulins: a two-step procedure using hydrophobic interaction chromatography and gel filtration. Journal of immunological methods. 1988;110(2):225-8.
132. Trindade IP, Diogo MM, Prazeres DM, Marcos JC. Purification of plasmid DNA vectors by aqueous two-phase extraction and hydrophobic interaction chromatography. Journal of Chromatography A. 2005;1082(2):176-84.
133. Diogo MM, Ribeiro S, Queiroz J, Monteiro G, Perrin P, Tordo N, et al. Scale-up of hydrophobic interaction chromatography for the purification of a DNA vaccine against rabies. Biotechnology Letters. 2000;22(17):1397-400.
134. Diogo M, Queiroz J, Monteiro G, Martins S, Ferreira G, Prazeres D. Purification of a cystic fibrosis plasmid vector for gene therapy using hydrophobic interaction chromatography. Biotechnology and bioengineering. 2000;68(5):576-83.
135. Melander W, Horváth C. Salt effects on hydrophobic interactions in precipitation and chromatography of proteins: an interpretation of the lyotropic series. Archives of biochemistry and biophysics. 1977;183(1):200-15.
136. Geng X, Guo LA, Chang J. Study of the retention mechanism of proteins in hydrophobic interaction chromatography. Journal of Chromatography A. 1990;507:1-23.
137. Lienqueo ME, Mahn A, Salgado JC, Asenjo JA. Current insights on protein behaviour in hydrophobic interaction chromatography. Journal of Chromatography B. 2007;849(1-2):53-68.
138. Privalov PL, Gill SJ. Stability of protein structure and hydrophobic interaction. Advances in protein chemistry. 39: Elsevier; 1988. p. 191-234.
139. Dill KA. Dominant forces in protein folding. Biochemistry. 1990;29(31):7133-55.
140. Zhang Y, Cremer PS. Interactions between macromolecules and ions: the Hofmeister series. Current opinion in chemical biology. 2006;10(6):658-63.
141. Xia F, Nagrath D, Garde S, Cramer SM. Evaluation of selectivity changes in HIC systems using a preferential interaction based analysis. Biotechnology and

bioengineering. 2004;87(3):354-63.
142. Szepesy L, Rippel G. Effect of the characteristics of the phase system on the retention of proteins in hydrophobic interaction chromatography. Journal of Chromatography A. 1994;668(2):337-44.
143. Hjertén S, Rosengren J, Sven P. Hydrophobic interaction chromatography: The synthesis and the use of some alkyl and aryl derivatives of agarose. Journal of Chromatography A. 1974;101(2):281-8.
144. Perkins TW, Mak DS, Root TW, Lightfoot EN. Protein retention in hydrophobic interaction chromatography: modeling variation with buffer ionic strength and column hydrophobicity. Journal of Chromatography A. 1997;766(1-2):1-14.
145. Roettger BF, Myers JA, Ladisch MR, Regnier FE. Adsorption phenomena in hydrophobic interaction chromatography. Biotechnology progress. 1989;5(3):79-88.
146. Pedro A, Oppolzer D, Bonifacio M, Maia C, Queiroz J, Passarinha L. Evaluation of Mut S and Mut+ Pichia pastoris strains for membrane-bound catechol-O-methyltransferase biosynthesis. Applied biochemistry and biotechnology. 2015;175(8):3840-55.
147. Arachea BT, Sun Z, Potente N, Malik R, Isailovic D, Viola RE. Detergent selection for enhanced extraction of membrane proteins. Protein expression and purification. 2012;86(1):12-20.
148. Pandey A, Shin K, Patterson RE, Liu X-Q, Rainey JK. Current strategies for protein production and purification enabling membrane protein structural biology. Biochemistry and Cell Biology. 2016;94(6):507-27.
149. Timmins P, Leonhard M, Weltzien H, Wacker T, Welte W. A physical characterization of some detergents of potential use for membrane protein crystallization. Febs Letters. 1988;238(2):361-8.
150. Harrison ST. Bacterial cell disruption: a key unit operation in the recovery of intracellular products. Biotechnology advances. 1991;9(2):217-40.
151. Boettner M, Prinz B, Holz C, Stahl U, Lang C. High-throughput screening for expression of heterologous proteins in the yeast Pichia pastoris. Journal of Biotechnology. 2002;99(1):51-62.
152. Passarinha L, Bonifacio M, Queiroz J. Comparative study on the interaction of recombinant human soluble catechol-O-methyltransferase on some hydrophobic adsorbents. Biomedical Chromatography. 2007;21(4):430-8.
153. Santos FM, Pedro AQ, Soares RF, Martins R, Bonifácio MJ, Queiroz JA, et al. Performance of hydrophobic interaction ligands for human membrane-bound catechol-O-methyltransferase purification. Journal of separation science. 2013;36(11):1693-702.
154. Mahn A, Lienqueo ME, Asenjo JA. Optimal operation conditions for protein

separation in hydrophobic interaction chromatography. Journal of Chromatography B. 2007;849(1-2):236-42.

155. Sousa A, Passarinha L, Rodrigues L, Teixeira J, Mendonça A, Queiroz J. Separation of different forms of proteose peptone 3 by hydrophobic interaction chromatography with a dual salt system. Biomedical Chromatography. 2008;22(5):447-9.

156. Passarinha L, Bonifácio M, Soares-da-Silva P, Queiroz J. A new approach on the purification of recombinant human soluble catechol-O-methyltransferase from an Escherichia coli extract using hydrophobic interaction chromatography. Journal of Chromatography A. 2008;1177(2):287-96.

157. Senczuk AM, Klinke R, Arakawa T, Vedantham G, Yigzaw Y. Hydrophobic interaction chromatography in dual salt system increases protein binding capacity. Biotechnology and bioengineering. 2009;103(5):930-5.

158. Oscarsson S. Influence of salts on protein interactions at interfaces of amphiphilic polymers and adsorbents. Journal of Chromatography B: Biomedical Sciences and Applications. 1995;666(1):21-31.

159. Machold C, Deinhofer K, Hahn R, Jungbauer A. Hydrophobic interaction chromatography of proteins: I. Comparison of selectivity. Journal of Chromatography A. 2002;972(1):3-19.

Appendix 1. Poster presentation at *10º Encontro Nacional de Cromatografia*, Bragança, Portugal (2017): Diogo P. Monteiro, Diana R. Duarte, Fátima M. Santos, Cláudio J. Maia, Luís A.

Passarinha, Design of an one-step platform purification of STEAP1 using Octyl-Sepharose.

CICS-UBI
Centro de Investigação em Ciências da Saúde
Health Sciences Research Centre

FACULDADE CIÊNCIAS DA SAÚDE

Design of an one-step platform purification of STEAP1 using octyl-sepharose

Diogo P. Monteiro[1], Diana R. Duarte[1], Fátima M. Santos[1,2], Cláudio J. Maia[1], Luís A. Passarinha[1,2]

[1] CICS-UBI – Health Sciences Research Centre, University of Beira Interior, Covilhã, Portugal.
[2] Laboratory of Pharmacology and Toxicology – UBIMedical, University of Beira Interior, Covilhã, Portugal

Introduction

Prostate cancer (PCa) is one of the most lethal and prevalent carcinoma among elder men worldwide [1]. Six transmembrane epithelial antigen of the prostate 1 (STEAP1) is a transmembrane protein whose high expression levels were correlated with PCa. STEAP1 may take part in intracellular and intercellular communication in cancer cells by modulating cell proliferation and tumor invasiveness through its potential activity as ion channel or transporter [2]. So, STEAP1 purification is crucial to further functional studies and 3D structure characterization.

Aim

Evaluate the performance of Octyl-Sepharose matrice with STEAP1 *Pichia Pastoris* lysates in order to purify considerable levels of the target protein.

Methodology

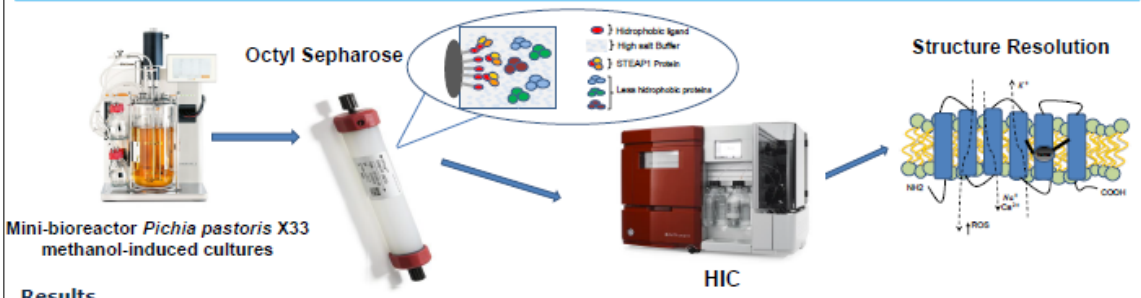

Results

Table 1. Summary of salt and Triton X-100 concentrations applied, respectively, in retention and detergent gradient onto a Octyl-Sepharose support.

	[Phosphate Buffer] (mM)	Solubilization with Triton X-100 (0.1%)	STEAP1 retention	STEAP1 Elution Behaviour	
				Phosphate Buffer (50 mM)	Triton X-100 (%)
Chromatographic methodologies	1000	+	+++	-	0 - 1
	700	+	+	-	0 – 1
	650	-	+	-	0 – 1
	500	-	+	-	0 – 1
	400	-	-	+	0
	300	-	-	+	0
	250	-	-	+++	0

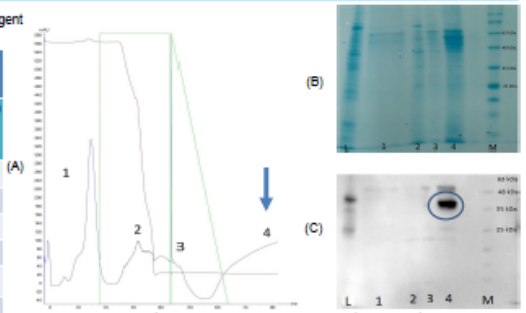

Figure 1 – (A) Chromatographic profile of STEAP1 isolation on Octyl-Sepharose. Adsorption was performed at 1000 mM Phosphate Buffer pH 8,0; followed by 50 mM Phosphate Buffer step. Elution was performed with a linear gradient of 1% Triton. Arrow indicate the presence of STEAP1. Analysis of chromatographic fraction by (B) SDS-Page and (C) Western Blot.

Conclusions

- The complete adsorption of STEAP1 was achieved on Octyl-Sepharose at phosphate buffer (1M), after its solubilization with 1% Triton, which shows the exposition of membrane binding domains of STEAP1 to octyl ligand requires high salt concentrations.
- Detergents are required to promote the elution of this membrane protein.
- Although successful applications of HIC in the purification of integral membrane proteins solubilized with detergents are uncommon, our results indicate that traditional hydrophobic matrices can open a promising alternative for the isolation of STEAP1.

References

[1] I.M. Gomes, P. Arinto, C. Lopes et al., Urologic Oncology Seminars and Original Investigation 2014, 53, 23-29.
[2] J.B. Ferreira, J.P. Pais, M.M. Santos et al., Current Cancer Drug Targets 2017, 17.

FCT COMPETE 2020 PORTUGAL 2020